

# **ROLE OF MAGNETIC RESONANCE VENOGRAM, DIFFUSION AND SUSCEPTIBILITY WEIGHTED IMAGING IN DIAGNOSIS OF CEREBRAL VENOUS THROMBOSIS**

By  
**DR. AMBUJ**



**DISSERTATION SUBMITTED TO SRI DEVARAJ URS  
ACADEMY OF HIGHER EDUCATION AND RESEARCH,  
KOLAR, KARNATAKA**

**In partial fulfillment of the requirements for the degree of**

**DOCTOR OF MEDICINE  
IN  
RADIODIAGNOSIS**

**Under the Guidance of  
Dr. ANIL KUMAR SAKALECHA, MD  
Professor**



**DEPARTMENT OF RADIODIAGNOSIS,  
SRI DEVARAJ URS MEDICAL COLLEGE & RESEARCH  
CENTER,  
TAMAKA, KOLAR-563101  
2016**

## **DECLARATION BY THE CANDIDATE**

I hereby declare that this dissertation entitled “**ROLE OF MAGNETIC RESONANCE VENOGRAM, DIFFUSION AND SUSCEPTIBILITY WEIGHTED IMAGING IN DIAGNOSIS OF CEREBRAL VENOUS THROMBOSIS**” is a bonafide and genuine research work carried out by me under the guidance of **Dr. ANIL KUMAR SAKALECHA**, M.D, Professor Department of Radiodiagnosis, Sri Devaraj Urs Medical College, Kolar, in partial fulfillment of University regulation for the award “**M.D. DEGREE IN RADIODIAGNOSIS**”, the examination to be held in April, 2016 by SDUAHER. This has not been submitted by me previously for the award of any degree or diploma from the university or any other university.

**Date:**

**Place: Kolar**

**Dr. AMBUJ**

Post Graduate.  
Department of Radiodiagnosis.  
Sri Devaraj Urs Medical College  
Tamaka  
Kolar

## **CERTIFICATE BY THE GUIDE**

This is to certify that the dissertation entitled “**ROLE OF MAGNETIC RESONANCE VENOGRAM, DIFFUSION AND SUSCEPTIBILITY WEIGHTED IMAGING IN DIAGNOSIS OF CEREBRAL VENOUS THROMBOSIS**” is a bonafide research work done by **Dr. AMBUJ**, under my direct guidance and supervision at Sri Devaraj Urs Medical College, Kolar, in partial fulfillment of the requirement for the degree of “**M.D. IN RADIO DIAGNOSIS**”.

**Date:**

**Place: Kolar**

**Dr. ANIL KUMAR SAKALECHA, MD**

Professor

Department of Radiodiagnosis

Sri Devaraj Urs Medical College,

Tamaka

Kolar

**ENDORSEMENT BY THE HEAD OF THE**  
**DEPARTMENT AND PRINCIPAL**

This is to certify that the dissertation entitled “**ROLE OF MAGNETIC RESONANCE VENOGRAM, DIFFUSION AND SUSCEPTIBILITY WEIGHTED IMAGING IN DIAGNOSIS OF CEREBRAL VENOUS THROMBOSIS**” is a bonafide research work done by **Dr. AMBUJ** under the direct guidance and supervision of **Dr. ANIL KUMAR SAKALECHA**, professor Department of Radiodiagnosis, Sri Devaraj Urs Medical College, Kolar, in partial fulfillment of University regulation for the award of “**M.D. IN RADIODIAGNOSIS**”.

**Dr. PURNIMA HEGDE MD,**

Professor & HOD

Department Of Radiodiagnosis,

Sri Devaraj Urs Medical College,

Tamaka, Kolar

**Date:**

**Place: Kolar**

**Dr. RANGANATH.B.G**

Principal,

Sri Devaraj Urs Medical College

Tamaka, Kolar

**Date:**

**Place: Kolar**

## **ETHICAL COMMITTEE CERTIFICATE**

This is to certify that the Ethical committee of Sri Devaraj Urs Medical College, Tamaka,

Kolar has unanimously approved

***Dr. AMBUJ***

***Post-Graduate student in the subject of***

***RADIODIAGNOSIS at Sri Devaraj Urs Medical College, Kolar***

***to take up the Dissertation work entitled***

**“ROLE OF MAGNETIC RESONANCE VENOGRAM, DIFFUSION AND  
SUSCEPTIBILITY WEIGHTED IMAGING IN DIAGNOSIS OF  
CEREBRAL VENOUS THROMBOSIS”**

***to be submitted to the***

**SRI DEVARAJ URS ACADEMY OF HIGHER EDUCATION AND  
RESEARCH CENTER, TAMAKA, KOLAR, KARNATAKA,**

**Member Secretary**

Sri Devaraj Urs Medical College  
Tamaka, Kolar

## **COPY RIGHT**

### **DECLARATION BY THE CANDIDATE**

I, hereby declare that the Sri Devaraj Urs Academy of Higher Education and Research, Kolar, Karnataka, shall have the right to preserve, use and disseminate this dissertation / thesis in print or electronic format for academic/research purpose.

**Date:**  
**Place: Kolar**

**Dr.AMBUJ**

## **ACKNOWLEDGEMENT**

I owe debt and gratitude to my parents **Shri VIJAY KUMAR SHRIVASTAV and Smt. MALA SHRIVASTAV**, along with my sister **Dr.VARTIKA** and my wife **Ar. RESHMI SHRIVASTAV** for their moral support and constant encouragement during the study.

With humble gratitude and great respect, I would like to thank my teacher, mentor and guide, **Dr. ANIL KUMAR SAKALECHA**, Professor, Department of Radiodiagnosis, Sri Devaraj Urs Medical College and Research Institute, Kolar, for his able guidance, constant encouragement, immense help and valuable advices which went a long way in moulding and enabling me to complete this work successfully.

I have great pleasure in expressing my deep sense of gratitude to **Dr. PURNIMA HEGDE**, Professor and Head, Department of Radiodiagnosis, Sri Devaraj Urs Medical College and Research Institute, Kolar. Without her initiative and constant encouragement this study would not have been possible. Her vast experience, knowledge, able supervision and valuable advices have served as a constant source of inspiration during the entire course of my study.

I would like to express my sincere thanks to **Dr. PATTIBHARAMAN**, Professor, Department of Radiodiagnosis, Sri Devaraj Urs Medical College for his valuable support, guidance and encouragement throughout the study.

I would like to thank **Dr. RACHE GOWDA, Dr.NABKUMAR SINGH and Dr.ASHWATHNARAYANASWAMY**, Professors, Department of Radiodiagnosis, Sri Devaraj Urs Medical College and Research Institute, Kolar, for their constant guidance and encouragement during the study period.

I also thank **Dr. NAVEEN G NAIK, Dr.JAGADISH, Dr.VINAY KK and Dr. KUKU MARIAM SURESH**, Assistant professors, Department of Radiodiagnosis, Sri Devaraj Urs Medical College, Kolar for their support.

I am thankful to my fellow **colleagues**, for having rendered all their cooperation and help to me during my study.

My sincere thanks to **Mrs.Veena** along with rest of the **staff's** and **Mr. Chandrashekar, Mr. Aleem, Mr. Mateen, Mr.Gurumoorthi, along** with rest of the technicians of Department of Radiodiagnosis, Sri DevarajUrs Medical College and Research Institute, Kolar.

My sincere thanks to all the patients and their families who formed the backbone of this dissertation. My sincere thanks to the Principal, SDUMC, KOLAR and the Medical Superintendent, R.L. Jalappa Hospital and Research centre (affiliated to SDUMC).

Last but not least I would be failing in my duty if I do not express my gratefulness to the almighty that has helped me to successfully complete this study.

**Dr. AMBUJ**



## **LIST OF ABBREVIATIONS**

CVT – Cerebral Venous Thrombosis

MRI – Magnetic resonance imaging

MRV- Magnetic resonance venogram

DWI - Diffusion weighted imaging

SWI- Susceptibility weighted imaging

MSE- Magnetic susceptibility effect

ADC – Apparent diffusion coefficient

T1 W – T1 Weighted

T2 W – T2 Weighted

FLAIR – Fluid- attenuated inversion recovery

HSI – High signal intensity

TOF – Time of flight

MIP – Maximum intensity projection

SSS - Superior sagittal sinus

ISS – Inferior sagittal sinus

SS – Straight sinus

TS – Transverse sinus

ROI – Region of interest

IV – Intravenous

## **ABSTRACT**

### **Introduction**

Cerebral venous thrombosis (CVT) is an uncommon and sometimes critical disease, especially in untreated patients. CVT is an elusive diagnosis because of its nonspecific presentation and its numerous predisposing causes. Accurate diagnosis is difficult but important because effective therapies, including anticoagulants and intrasinus thrombolysis are available. Patients with cerebral venous thrombosis often make dramatic recoveries after anticoagulation. For this reason, accurate and early diagnosis is important and critical.

### **Aims:**

1. To study the extent of venous sinus involvement and associated cerebral parenchymal changes on MR venogram.
2. To study the pattern of diffusion weighted images and ADC mapping in patients with cerebral venous thrombosis.
3. To study the role of susceptibility weighted images in patients with cerebral venous thrombosis

**Materials and Methods:** Study was conducted on 34 patients diagnosed to have cerebral venous thrombosis on imaging.

**Results:**

Imaging analyses of 34 patients (19 females, 15 males, and age range 19-75 years) were done. Thrombus on MRV was seen as loss of high flow signal from the sinus in cases of complete occlusion of the sinus and frayed or patchy flow signal in the cases of non-occlusive thrombus. 16 patients with hemorrhagic infarct showed heterogeneous signal intensity on DWI and blooming on SWI sequence. 13 patients with non-hemorrhagic infarct showed multifocal high signal intensities in DWI with variable ADC values and no blooming on SWI. 5 patients with intracerebral hematoma showed areas of blooming on SWI and no restriction on DWI, corresponding ADC values were variable.

**Conclusion:**

MR venogram, diffusion and susceptibility weighted imaging can be used to evaluate the extent of thrombus, detect intracerebral hematoma, hemorrhagic and non-hemorrhagic infarcts and deliver time-saving information for early diagnosis of CVT.

## **TABLE OF CONTENTS**

<b>1. INTRODUCTION .....</b>	<b>01</b>
<b>2. AIMS AND OBJECTIVES.....</b>	<b>02</b>
<b>3. REVIEW OF LITERATURE.....</b>	<b>03</b>
<b>4. MATERIALS AND METHODS.....</b>	<b>58</b>
<b>5. RESULTS .....</b>	<b>60</b>
<b>6. DISCUSSION.....</b>	<b>72</b>
<b>7. CONCLUSION .....</b>	<b>77</b>
<b>8. SUMMARY .....</b>	<b>79</b>
<b>9. BIBLIOGRAPHY.....</b>	<b>81</b>
<b>10.ANNEXURE 1.....</b>	<b>90</b>
<b>11.ANNEXURE 2.....</b>	<b>92</b>
<b>12.ANNEXURE 3.....</b>	<b>95</b>

## **LIST OF FIGURES**

<b>LIST OF FIGURES</b>		
<b>SL. NO.</b>	<b>NAME</b>	<b>PAGE NO.</b>
1	POST SEGMENTATION MR VENOGRAPHIC MIP IMAGES OF DEEP VENOUS SYSTEM	13
2	SUPERFICIAL CORTICAL VEINS ON POST SEGMENTATION MR VENOGRAPHIC MIP IMAGES	16
3	MAJOR DURAL SINUSES WITH MR VENOGRAPHIC MIP IMAGES	19
4	POST SEGMENTATION MR VENOGRAPHIC MIP IMAGES DEMONSTRATING CAVERNOUS SINUSES	21
5	INFRATENTORIAL VENOUS SINUSES	23
6	T1-WEIGHTED IMAGES IN THROMBOSIS	32
7	RECONSTRUCTED SAGITTAL CT-IMAGES OF SUPERIOR SAGITTAL SINUS THROMBOSIS WITH BILATERAL PARASAGITTAL HEMORRHAGE	33
8	SAGITTAL CT RECONSTRUCTION DEMONSTRATES FILLING DEFECT IN THE STRAIGHT SINUS AND THE VEIN OF GALEN	34
9	INFARCTION IN THE AREA OF THE VEIN OF LABBE	35
10	AXIAL COMPUTED-TOMOGRAPHY SCAN DEMONSTRATING INTRALUMINAL HYPERDENSITY OF CLOT IN SUPERIOR SAGITTAL SINUS WALL, CORTICAL VEINS OF RIGHT FRONTAL REGIONS	36
11	STAGES OF ISCHEMIC DAMAGE TO BRAIN TISSUE	41
12	SEX WISE DISTRIBUTION	60
13	AGE AND SEX WISE DISTRIBUTION	61
14	CAUSES OF CEREBRAL VENOUS THROMBOSIS	62
15	CLINICAL HISTORY IN PATIENTS OF CEREBRAL VENOUS THROMBOSIS	63
16	EXTENT OF THE THROMBOSIS	64
17	ASSOCIATED MANIFESTATIONS	65

18	SINUSES INVOLVED	66
19	DWI, ADC, SWI, MRV IMAGES SHOWING HEMORRHAGIC INFARCT IN LEFT TEMPOROPARIETAL REGION AND THROMBOSIS OF SUPERIOR SAGITTAL, TRANSVERSE AND SIGMOID SINUSES.	67
20	SWI, DWI, MRV IMAGES SHOWING HEMORRHAGIC INFARCTS IN RIGHT FRONTO-PARIETAL LOBES AND THROMBOSIS OF SUPERIOR SAGITTAL, RIGHT TRANSVERSE, SIGMOID SINUS, DISTAL STRAIGHT SINUS AND INTERNAL JUGULAR VEIN.	68
21	DWI, ADC, SWI, MRV IMAGES SHOWING HEMORRHAGIC INFARCT IN RIGHT INFERIOR TEMPORAL LOBE AND THROMBOSIS OF SUPERIOR SAGITTAL, RIGHT TRANSVERSE, SIGMOID SINUS AND LEFT PROXIMAL TRANSVERSE AND SIGMOID SINUSES.	69
22	DWI, ADC, SWI, MRV IMAGES SHOWING HEMORRHAGIC INFARCT IN LEFT PARIETAL LOBE AND THROMBOSIS OF SUPERIOR SAGITTAL, RIGHT TRANSVERSE, SIGMOID SINUSES AND PROXIMAL IJV.	70
23	DWI, SWI AND MRV IMAGES SHOWING HEMORRHAGES IN BILATERAL FRONTAL LOBES AND THROMBOSIS OF ANTERIOR SUPERIOR SAGITTAL SINUS AND HYPOPLASTIC LEFT TRANSVERSE SINUS	71

## **LIST OF TABLES**

<b>LIST OF TABLES</b>		
<b>SL. NO.</b>	<b>NAME</b>	<b>PAGE NO.</b>
1	RISK FACTORS FOR CEREBRAL VENOUS THROMBOSIS	24
2	CLINICAL PRESENTATION OF CVT	27
3	SEX WISE DISTRIBUTION IN PATIENTS WITH CEREBRAL VENOUS THROMBOSIS	60
4	AGE AND SEX WISE DISTRIBUTION IN PATIENTS WITH CEREBRAL VENOUS THROMBOSIS	61
5	DISTRIBUTION OF PATIENTS DEPENDING ON THE CAUSE IN PATIENTS WITH CEREBRAL VENOUS THROMBOSIS	62
6	DISTRIBUTION OF PATIENTS BASED ON CLINICAL HISTORY IN PATIENTS WITH CEREBRAL VENOUS THROMBOSIS	63
7	DISTRIBUTION OF PATIENTS WITH CEREBRAL VENOUS THROMBOSIS DEPENDING ON THE EXTENT OF THROMBOSIS (NO.OF SINUSES INVOLVED IN EACH PATIENT)	64
8	DISTRIBUTION OF PATIENTS WITH CEREBRAL VENOUS THROMBOSIS ACCORDING TO ASSOCIATED MANIFESTATIONS	65
9	DISTRIBUTION OF SINUSES INVOLVED IN PATIENTS OF CEREBRAL VENOUS THROMBOSIS	66

## **INTRODUCTION**

Cerebral venous thrombosis (CVT) is an uncommon and sometimes critical disease, especially in untreated patients.

CVT is a cause of stroke with obscure pathophysiologic properties that differ from arterial stroke. Its main mechanisms of pathophysiology are the breakdown of the blood-brain barrier and the coexistence of cytotoxic and vasogenic edema.

Cerebral venous thrombosis differs from arterial infarction in several ways. First, the clinical presentation is variable and may range from subacute headache, raised intracranial pressure to severe multifocal deficits, seizures and coma<sup>1</sup>.

Accurate diagnosis is difficult but important because effective therapies are available. Patients with cerebral venous thrombosis often make dramatic recoveries and for this reason accurate diagnosis is important and critical.

Diffusion weighted imaging with ADC mapping, susceptibility weighted imaging and MR venogram can be used to evaluate extent of thrombus, discriminate between different types of edema, detect presence of hemorrhage and deliver time-saving information for early diagnosis of CVT.



## **AIMS AND OBJECTIVES**

1. To study the extent of venous sinus involvement and associated cerebral parenchymal changes on MR venogram.
2. To study the pattern of diffusion weighted images and ADC mapping in patients with cerebral venous thrombosis.
3. To study the role of susceptibility weighted images in patients with cerebral venous thrombosis

# **REVIEW OF LITERATURE**

## **HISTORICAL REVIEW OF MRI**

MRI is based on the principles of nuclear magnetic resonance (NMR), a spectroscopic technique used by scientists to obtain microscopic chemical and physical information about molecules. The technique was called magnetic resonance imaging (NMRI) because of the negative connotations associated with the word nuclear in the late 1970's

The Concept of Nuclear Magnetic Resonance (NMR) was described by Dutch Physicist C.J Gorter in 1936. Felix Bloch and Edward Purcell, both of whom were awarded Nobel Prize in 1952, discovered the magnetic resonance phenomenon independently in 1946. In the period between 1950 and 1970, NMR was developed and used for chemical and physical molecular analysis.

In 1971 Raymond Damadian was among the first to suggest the use of NMR in medical diagnosis and he showed that the nuclear magnetic relaxation times of tissues and tumors differed, thus motivating scientists to consider magnetic resonance for the detection of disease<sup>2</sup>. Lauterbur published the first NMR image on small test tube samples in 1972 at Stony Brook, New York. He was able to generate the first two-dimensional NMR image of proton density and spin lattice relaxation time. Lautenber coined the term "Zeugmatography" (From Greek Zeugma, meaning that which joins together) for his technique. He used a back projection technique similar to that used in CT<sup>3</sup>. In 1975 Richard Ernst proposed magnetic resonance imaging using phase and frequency encoding, and the Fourier Transform. This technique is the basis of current MRI techniques<sup>4</sup>.

It was in 1976 and 1977, when first images of human anatomy were produced by groups at Nottingham University. In 1977, Raymond Damadian produced whole body image using field-focusing nuclear magnetic resonance. In this same year, Peter Mansfield developed the echo-planar imaging (EPI) technique<sup>5</sup>. This technique will be developed in later years to produce images at video rates (30ms/image).

The multiplanar facility of MRI (Magnetic Resonance Imaging) was first demonstrated in 1980 by Hawkes, who also reported the first intracranial pathology. Edelstein and coworkers demonstrated imaging of the body using high field (1.5T) whole body magnets. In 1987 echo-planar imaging was used to perform real-time movie imaging of a single cardiac cycle<sup>6</sup>. In this same year Charles Dumoulin was perfecting magnetic resonance angiography (MRA), which allowed imaging of flowing blood without the use of contrast agents<sup>7</sup>.

In 1991, Richard Ernst was rewarded for his achievements in pulsed Fourier Transform NMR and MRI with Nobel Prize in Chemistry. In 1992 functional MRI (fMRI) was developed<sup>8</sup>. The development of fMRI opened up a new application for EPI in mapping the regions of the brain responsible for thought and motor control. In 1994, researchers at the State University of New York at Stony Brook and Princeton University demonstrated the imaging of hyperpolarized <sup>129</sup>Xe gas for respiration studies<sup>9</sup>.

Interventional MRI was first shown by Lufkin et al in 1995 and hold great promise for diagnosing and treating patients within a single visit. Functional MR of brain which uses endogenous blood oxygen level dependent (BOLD) changes to map activities such as vision, motion and even memory formation was introduced by Ogawa et al in 1992 and developed by Rosen et al. New parallel encoding methods used with phased array radiofrequency coils such as

SMASH introduced by Sodickson et al in 1997 and SENSE introduced by Pruessmann et al in 1999 are changing the rules of imaging speed with MRI. As we enter twenty first century MRI and spectroscopy development is increasing pace and it is anticipated that this will continue with vigour<sup>10</sup>.

MR imaging is currently the diagnostic study of choice in CVT because of its capacity to visualize flow, thrombus, infarction, and any underlying abnormality<sup>11</sup>.

## **BASIC MRI PHYSICS**

Magnetic resonance describes the phenomenon whereby the nuclei of certain atoms, when placed in magnetic field, absorb and emit energy of a specific frequency. The spectrum of absorbed or emitted energy depends upon the nucleus under observation and its chemical environment.

The nuclei for MRI are those which have an odd number of protons or neutrons and therefore possess a net charge and have angular momentum. Because of combination of charge and angular momentum, these nuclei behave as magnetic dipoles. Almost all images produced to date have been of nuclear magnetism of the hydrogen nucleus (or proton) which is a particularly favorable nucleus from the MRI standpoint, and is present in virtually all biological material. Other naturally occurring magnetic nuclei which are of interest include Phosphorous ( $^{31}\text{P}$ ), Sodium ( $^{23}\text{Na}$ ), Carbon ( $^{13}\text{C}$ ) and Potassium ( $^{39}\text{K}$ ). In addition, exogenous noble gases such as Helium ( $^3\text{He}$ ) and Xenon ( $^{129}\text{Xe}$ ) can be made sufficiently sensitive by polarization outside the magnet using laser techniques to allow imaging of airways and in case of Xenon, blood perfusion<sup>12</sup>.

The proton can be recharged as a small, freely suspended bar magnet spinning rapidly about its magnetic axis. When a group of protons are placed in a uniform magnetic field, their magnetic field, their magnetic moments experience a couple tending to turn them parallel to the direction of the field. In a strong magnetic field, more of these nuclear magnetic dipoles align with applied static magnetic field than against it. This produces net magnetization in the direction of field. The direction of the strong magnetic field conventionally defines the Z-axis, which is generally along the longitudinal axis of the patient in a typical MRI imaging machine. In an interventional open magnet the field is often in the vertical direction. In dedicated extremity and neonatal MR field is in the horizontal plane across the magnet<sup>12</sup>.

The electrical Principle of MRI is based on the Larmor frequency of hydrogen proton. Hydrogen has a solitary proton within its nucleus resulting in all hydrogen atoms having an inherent positive charge. When combined with the spinning movement of the proton, this positive charge results in the proton behaving as a tiny magnet with both positively and negatively charged poles. Normally, protons in the human body are randomly oriented. However, when subjected to strong external magnetic field, these protons equilibrate to a low energy state, aligning along the direction of the main magnetic field lines. When a RF pulse is generated at the appropriate frequency the atoms are excited to a higher energy state. After the RF pulse is removed, the protons relax back to their low energy state. The rate and nature of this relaxation is defined by the chemical, structural and local magnetic environment in which the protons are found.

The strong magnetic field, which must be homogenous over a volume large enough to contain the human body in an MRI imaging machine, is provided by a resistive, permanent or superconducting magnet. Magnetic field strengths are used for clinical imaging currently range from 0.02 Tesla (T) to 8T.

Because the nuclei are spinning, they respond to the magnetic couple like gyroscope and their axes are tilted so that they come to rotate at exactly the same frequency about the magnetic field; direction in a movement is known as 'precession'. The frequency of precession is directly proportional to the applied magnetic field for protons in a field of 1T; it is 42.6 MHz. This relationship is expressed as Larmor equation:

$$f = \gamma B$$

Where  $f$  is the resonant frequency,  $\gamma$  is the gyromagnetic ratio, and  $B$  is the applied field, there is strong interaction or resonant effect, providing that the frequency of the oscillation is equal to the precession frequency of the protons. This is called Magnetic Resonance and manifests itself in the following way: RF energy is absorbed from the transmitter coil which causes the motion of elementary magnets to be distributed so that the direction of the total nuclear magnetization is altered. The net magnetization along the Z-axis is deviated through an angle which depends upon the strength and duration of the pulse of the RF magnetic field  $90^\circ$  and  $180^\circ$  respectively. After the disturbance induced by the applied pulse or pulses, the magnetization returns to its equilibrium position along the z-axis in an exponential manner and as it does so, the changing magnetization induces a small voltage in receiver coil which placed next to patient<sup>12</sup>.

The electrical signal detected following an RF pulse is known as the free induction decay or FID, the magnitude and length of which is determined by the nuclear relaxation times which reflect molecular motion.

The first of these relaxation times,  $T_1$  or the longitudinal relaxation time, represents the time taken by the system of nuclei to return to thermal equilibrium after the RF pulse. The second or transverse relaxation,  $T_2$ , indicates the characteristic decay time of the FID and is due to the

irreversible dephasing of the initially coherent precession of nuclei which follows the RF pulse. In liquids or systems containing mobile protons,  $T_2/T_1$  is approximately unity, whereas in solids,  $T_2/T_1$  is very small. Unlike CT images in which contrast is determined by differences in one parameter (the linear X-ray attenuation coefficient  $\mu$ ), multiple parameters influence the MRI signal including nuclear (or proton) density,  $T_1$  and  $T_2$ . In human tissue  $T_1$  is usually 10 times longer than  $T_2$  meaning  $T_2$  decay occurs before  $T_1$  recovery although both processes are occurring together immediately after RF pulse is turned off. A local change in magnetic field homogeneity, e.g. due to local iron or deoxy-haemoglobin content, causes a reduction in  $T_2$  which is called  $T_2^*$ . In addition, flowing material within the image plane may alter contrast.  $T_1$  and  $T_2$  variations between tissues are usually more than variations in proton density so images with high dependence have greater contrast on  $T_1$  or  $T_2$  therefore<sup>12</sup>.

## **VARIOUS PULSE SEQUENCES**

Several different pulse sequences and functional imaging derived from combination of pulse sequences have been developed and are generally available on most commercial MR imaging systems<sup>13-15</sup>. These include:

- a) Partial saturation (PS)
- b) Spin echo (SE)
- c) Inversion recovery
- d) Multiecho
- e) Calculated  $T_1$  and  $T_2$

## **LOCALIZATION OF MRI SIGNAL**

Each volume element in the body is therefore labeled by having different resonant frequency for protons within it. The resulting complicated FID signal is digitized and frequency analyzed in a computer using a mathematical technique known as *Fourier analysis*.

By using a series of phase encoding gradients of different strengths, the spatial distribution of signals along the perpendicular gradient direction can also be obtained. This is the basis of the widely employed *two-dimension (2D) Fourier transform* method imaging.

During imaging, an array of numbers is generated, each row of which correspond to each application of phase encoding gradient. This array of data, with  $k_x$  axes, is known as 'k-space' or spatial frequency space. Fourier transformation of the data in k-space gives rise to an MR image<sup>12</sup>.

## **INSTRUMENTATION**

All MRI scanners are constructed around magnets which may vary in field strength between 0.02 T and 8T, the principal benefit of higher field strength being on increased signal-to-noise ratio (SNR). The various instruments are explained below:

1. **MAGNET**: The static magnetic field is established by a large magnet that may be one of three types. In August of 1984, 147 clinical MRI sites were operating using a variety of magnet types.



Permanent magnets are currently under study and are being used by a few manufacturers. This is the simplest method for generating magnetic fields and has the advantage of limited fields external to the imaging system. However, the application of current permanent magnet technology to imaging applications is hampered by the extremely large size required (weighing on the order of 25,000 pounds), thermal instability, and the relatively poor uniformity (possibly corrected by the addition of shim coils) of the fields that are generated.

Resistive magnets are one type of electromagnet currently in use for imaging. These magnets are based on the well-known physics principle that current flowing through a wire will generate magnetic field about the wire. Resistive magnets generally consists of four to six coils of hollow copper tubing wound to roughly approximate the shape of a sphere.

2. GRADIENT COILS: Another integral part of the imaging system is the gradient coils. As stated earlier, for imaging purposes it is necessary to be able to selectively alter the magnetic field in one or more directions. To accomplish this task three separate coils, termed the x, y and z gradient coils, are present and are constructed so that passage of current through each of the coils will linearly alter the magnetic field in the directions controlled by the coils.
3. RADIOFREQUENCY TRANSMITTER/ RECEIVER COILS: The actual signal transmission and reception are accomplished through the use of a radiofrequency (RF) transmitter coupled to a transmitting coil or antenna within the imaging unit and a radiofrequency receiver coupled to a receiving coil or antenna also located in the imaging unit and positioned as close to the patient as possible for maximum sensitivity.

4. SHIM COILS: Another important part of the imaging system related to the magnet is the shim coils. Currently available magnets alone cannot provide the necessary uniformity for imaging. By placing coils of wire at various locations around the imaging area and carefully adjusting the amount of current flowing through each coil, the field uniformity and/ or direction can be corrected or “shimmed” so that variations of no more than a few parts per million are achieved.
5. COMPUTER: Finally, a powerful computer system with a large memory, temporary (disk) and permanent (magnetic tape) storage capabilities, an array processor, and a high quality multiformat imager are necessary to acquire, process, store, and display the large volume of data associated with the imaging process.
6. IMAGE DISPLAY: MRI is based on computer processing and depends on its powerful image manipulation ability. The primary clinical diagnosis is made by visual inspection of the displayed image. Hence, the quality of the image display and the ability of the operator to interact with the image are the two most critical factors in the success of this modality. In most clinical systems, the computer displays are used for two operations:
  - a) Performance of the clinical study- is primarily a matter of displaying textual information and numerical values.
  - b) Presentation of the final image- is concerned with the presentation of high resolution images with a large number of image points and often a wide intensity range.

## **ANATOMY OF NORMAL INTRACRANIAL VENOUS SYSTEM**

The intracranial venous system is a complex three-dimensional structure that is often asymmetric and considerably more variable than the arterial anatomy.

The cerebral venous system comprises of dural venous sinuses and cerebral veins.

### **Deep venous system**

The deep venous system is concerned with centripetal venous drainage of deep cerebral white matter and basal ganglia and, using a classification suggested by Lasjaunias, can be considered at two

Separate levels:

- 1) The internal cerebral vein, the basal vein (of Rosenthal)

And the great cerebral vein (of Galen).

- 2) The transcerebral venous system<sup>16</sup>.

These two levels operate in a hemodynamic balance such that some overlap and variation in their venous drainage is common.

### **Internal cerebral vein**

The paired internal cerebral veins are located near the midline within the tela choroidea in the roof of the third ventricle. The internal cerebral vein originates at the interventricular foramen of Monro where it is formed by the confluence of the septal, anterior caudate, ventricular, choroidal, and terminal (thalamostriate) subependymal veins, although anatomical variation in this region is common<sup>17</sup>. The internal cerebral veins run posteriorly to where they unite in the rostral part of the quadrigeminal cistern and form the great cerebral vein (of Galen).

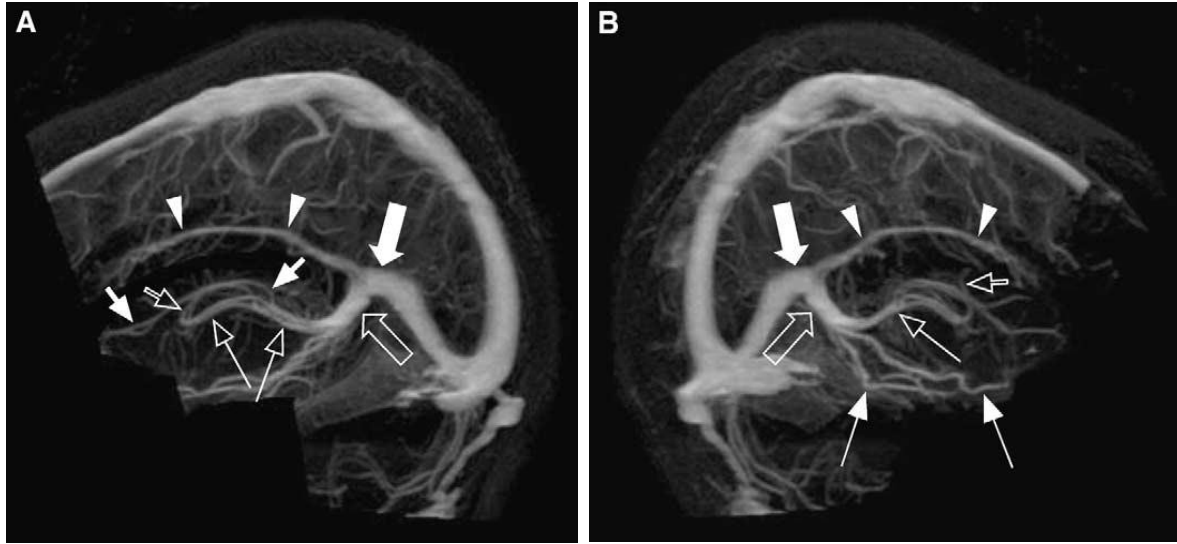


**FIG 1** Post segmentation MR venographic MIP images in (A) sagittal and (B) right posterior oblique projections demonstrate deep venous system structures, including variant anterior septal vein anatomy. The internal cerebral veins (open long arrows) collect the thalamostriate veins (open short arrows). The paired anterior septal veins (short arrows) join the main stem of the internal cerebral vein far beyond the foramen of Monro.

After coursing superolaterally around the midbrain, the basal veins (of Rosenthal) (long arrows) join the internal cerebral veins to form the great cerebral vein (of Galen) (open large arrow). The confluence of the great cerebral vein (of Galen) and inferior sagittal sinus (arrowheads) at the tentorial apex (large arrow) is also shown.

The septal vein drains the deep structures of the frontal lobes and courses around the anteromedial aspect of the lateral ventricle before passing posterior to the foramen of Monro to join the internal cerebral vein. The caudate nucleus is drained by several caudate veins, which drain into the thalamostriate vein or directly into the internal cerebral vein.

The thalamostriate vein drains the posterior frontal and anterior parietal lobes, caudate nucleus, and internal capsule, and is therefore usually a prominent tributary feeding the internal cerebral vein. Two choroidal veins (superior and inferior) that drain the choroid plexus empty either directly into the internal cerebral vein, or first to the thalamostriate vein.

The basal vein of Rosenthal originates deep within the sylvian fissure, near the medial part of the anterior temporal lobe, and receives veins draining the insula, cerebral peduncles, and multiple cortical (temporal) tributaries. The basal vein courses posteriorly at the base of the brain and curves around the cerebral peduncles to its junction with the great cerebral vein (of Galen) or internal cerebral vein. The basal vein has important anastomoses with its openings into the deep middle cerebral vein anteriorly, great cerebral vein (of Galen) posteriorly, and petrosal veins inferiorly.

The great cerebral vein (of Galen) is a short, unpaired, midline structure that curves posteriorly beneath the splenium of the corpus callosum. It unites with the inferior sagittal sinus at the tentorial apex and forms the straight sinus.

The transcerebral veins are a group of superficial and deep medullary veins that drain the cerebral hemispheric white matter. The transcerebral veins are typically not visualized, however, during angiography because of their small caliber unless certain conditions are met that alter their normal hemodynamic state.

## **SUPERFICIAL CEREBRAL VEINS**

The superficial cerebral veins course over the surface of the brain, draining the cortex and a portion of the subjacent white matter. Despite a highly variable appearance, several large cortical veins can often be identified individually and include :-

- (1) Superficial middle cerebral vein,
- (2) Superior anastomotic vein, and
- (3) Inferior anastomotic vein

The latter two anastomotic veins are often in a reciprocal relationship such that if one is dominant, the other is usually hypoplastic or absent.

The superficial middle cerebral vein runs anteriorly along the lateral (sylvian) fissure and receives smaller veins draining the lateral surface of the hemisphere. This large vein curves around the anterior temporal pole and drains either medially into the cavernous sinus or inferiorly into the pterygoid plexus. Anastomotic channels allow the superficial middle cerebral vein to drain in other directions. These include the superior anastomotic vein (of Trolard), which opens into the superior sagittal sinus, and the inferior anastomotic vein (of Labbe'), which opens into the transverse sinus. There are a variable number of other superiorly directed superficial cortical veins, often 10–12 in number, that also empty into the superior sagittal sinus along with the vein of Trolard.

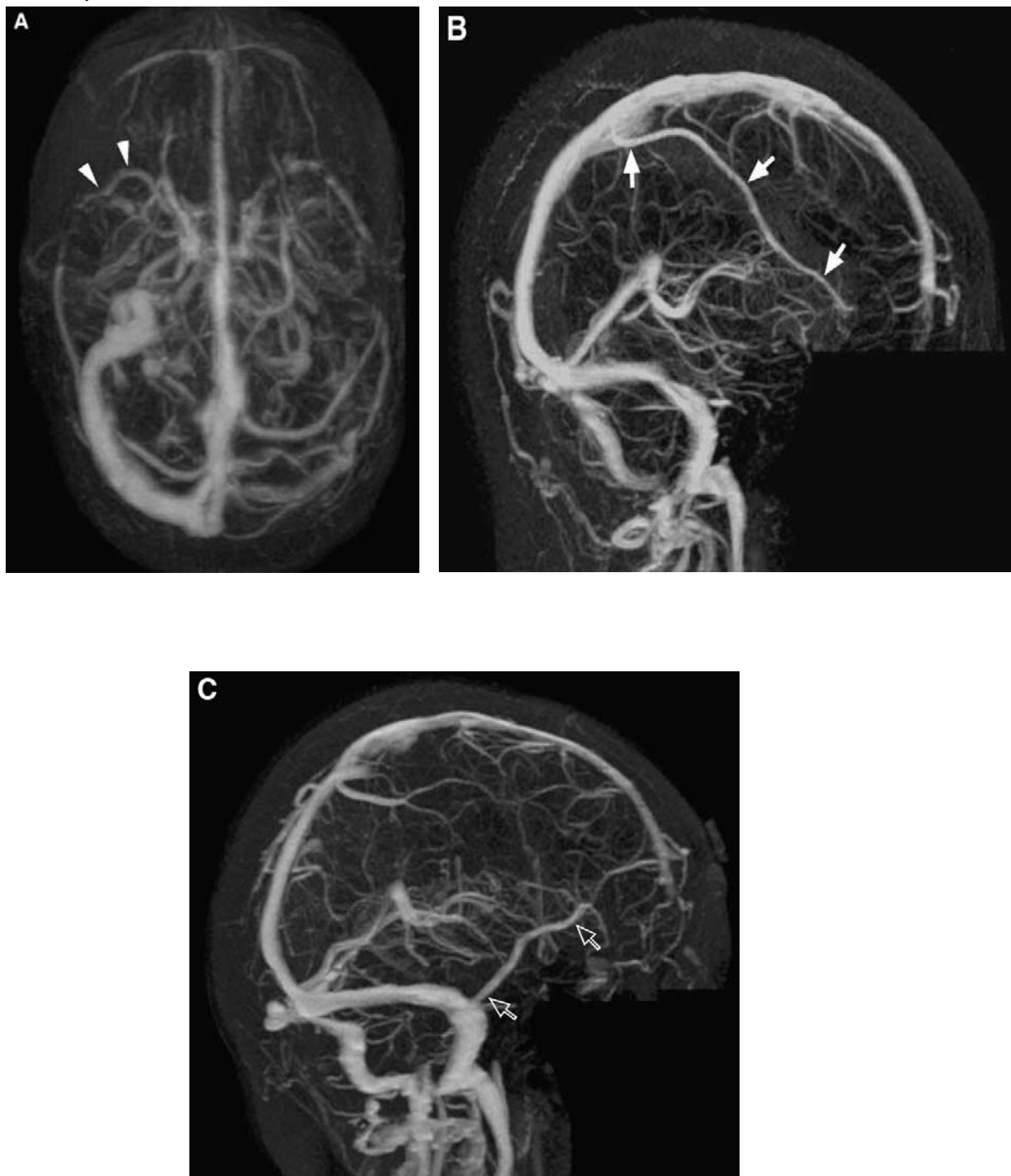


**FIG 2** - Three different patients in whom superficial cortical veins are noted on post segmentation MR venographic MIP images. (A) The superficial middle cerebral vein (arrowheads) drains anteromedially into the cavernous or sphenoparietal sinus on this submento-vertex view. (B) The superior anastomotic vein of Trolard (short arrows) opens superiorly into the superior sagittal sinus along with multiple superior superficial cortical veins. (C) The inferior anastomotic vein of Labbe (open short arrows) opens into the transverse sinus

## **DURAL VENOUS SINUSES**

The cerebral veins empty into the venous sinuses, from which blood eventually flows into the internal jugular veins. Dural venous sinuses are enclosed between the periosteal and meningeal layers of dura, and they lack valves.

### **SUPERIOR SAGITTAL SINUS**

It lies along the attached border of the falx cerebri and extends from the foramen caecum to the torcular Herophili. As it extends posteriorly, the superior sagittal sinus increases in caliber as it collects the superficial cerebral veins draining the cerebral convexities. Arachnoid granulations, contained within venous lacunae, are found protruding into the superior sagittal sinus along its course and may produce normal filling defects on imaging studies.

### **INFERIOR SAGITTAL SINUS**

It lies along the inferior free margin of the falx cerebri and drains the falx, anterior part of the corpus callosum, and medial aspects of the cerebral hemispheres. The inferior Sagittal sinus extends posteriorly and is joined by the great cerebral vein (of Galen) to form the straight sinus.

### **STRAIGHT SINUS**

It lies within the attachment of the falx cerebri and tentorium cerebelli. It runs posteroinferiorly, terminates at the internal occipital protuberance, and is usually continuous with the left transverse sinus. The union of the superior sagittal sinus, straight sinus, and transverse sinuses forms the torcular Herophili (confluence of sinuses), although the confluence is often asymmetric and quite variable in appearance<sup>18,19</sup>.



## **TRANSVERSE SINUSES**

It lies along the attached margin of the tentorium cerebelli within a groove on the occipital bone. Each transverse sinus courses anterolaterally and, on reaching the base of the petrous portion of the temporal bone, turns inferomedially to form the sigmoid sinus that lies in the sigmoid sulcus of the temporal bone. The transverse sinus receives several important veins from the inferolateral temporal occipital lobe, the cerebellum, and, when present, the anastamotic cortical vein of Labbe´.

The transverse sinuses are commonly asymmetric, with the right transverse sinus being dominant in the majority of cases. Other common variations include a unilateral atretic segment and normal intraluminal filling defects resulting from arachnoid granulations, similar to those seen in the superior sagittal sinus<sup>20,21,22</sup>.

## **SIGMOID SINUSES**

The sigmoid sinuses represent the anteroinferior continuation of the transverse sinuses and, in turn, drain into the jugular bulbs and terminate by becoming the internal jugular veins at the jugular foramen.

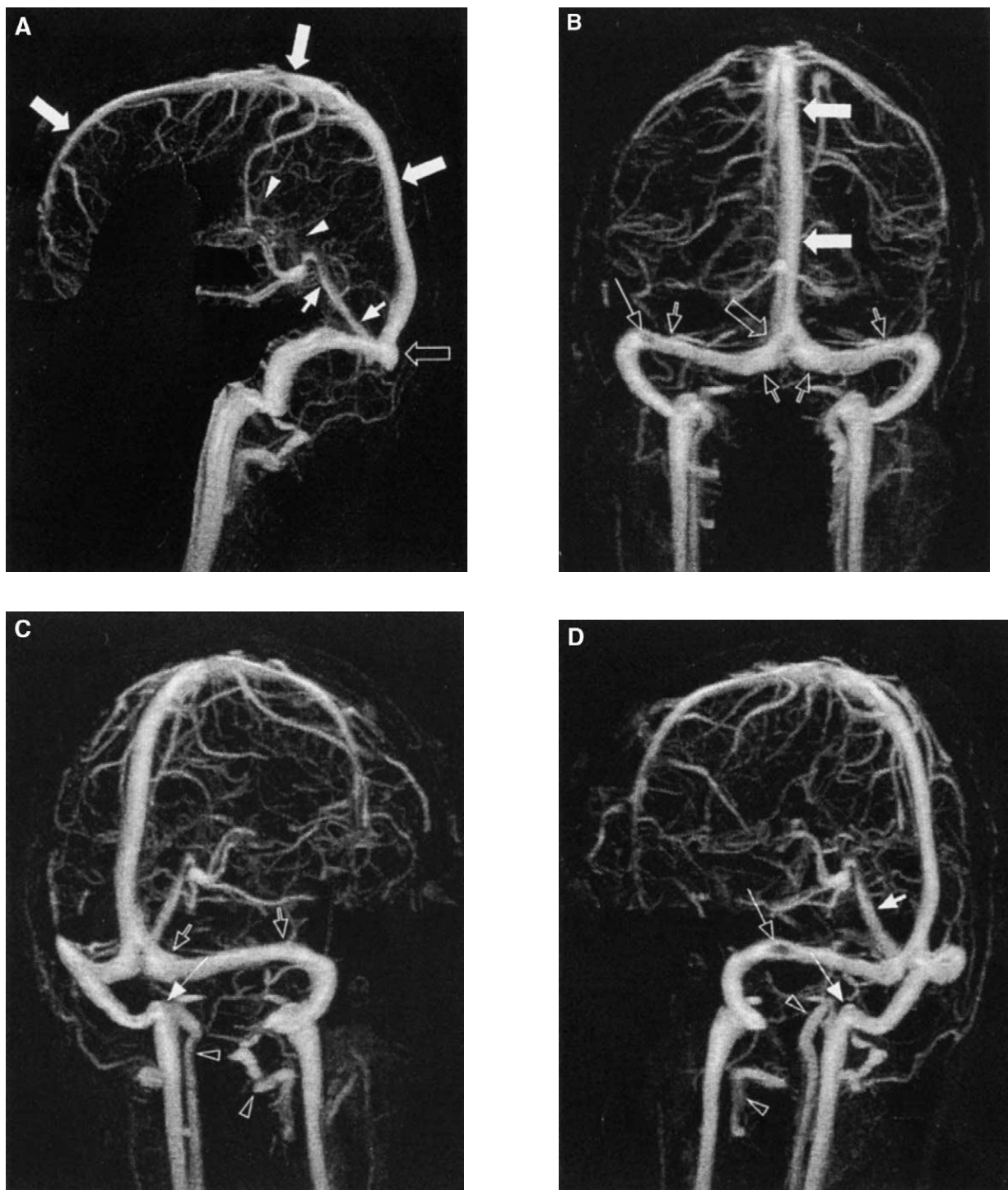


**FIG 3** - Visualization of the major dural sinuses with MR venographic MIP images in (A) sagittal, (B) antero-posterior, (C) right anterior oblique, and (D) left anterior oblique projections post segmentation to remove major arteries located at the skull base. The superior sagittal sinus (large arrows) becomes progressively larger as it courses posteriorly, and is joined by the straight sinus (short arrows) and transverse sinuses (open short arrows) at the confluence of sinuses (torcular Herophili) (open large arrow). The hypoplastic inferior sagittal sinus (arrowheads) and left jugular bulb (long arrow) are also labelled. A round intraluminal filling defect within the distal right transverse sinus represents a normal arachnoid granulation (open long arrow). Non excluded portions of the internal carotid and vertebral arteries (open arrowheads) are also visible on these views

## **CAVERNOUS SINUSES**

They are situated on each side of the sphenoid body and represent an important confluence of intracranial and extracranial venous structures. Each cavernous sinus is a multi-compartmental extradural space that extends from the superior orbital fissure to the petrous portion of the temporal bone. This sinus encloses the cavernous segment of the internal carotid artery and the abducens nerve, whereas the lateral wall of the sinus contains the oculomotor, trochlear, and ophthalmic division of the trigeminal nerves between its dural leaves.

## **SUPERIOR PETROSAL SINUS**

They extend from the posterior aspect of the cavernous sinus to the transverse sinus, running along the attachment of the tentorium cerebelli to the petrous part of the temporal bone.

## **INFERIOR PETROSAL SINUS**

The inferior petrosal sinus also extends from the posterior aspect of the cavernous sinus but runs posterolaterally in a groove along the petro-occipital fissure to usually terminate by joining the jugular bulb

## **SPHENOPARIETAL SINUS**

The sphenoparietal sinus lies along the lesser wing of sphenoid and drains usually the superficial middle cerebral (sylvian) vein into the cavernous sinus. Less common variations include the sphenoparietal sinus bypassing the cavernous sinus to drain into either the pterygoid plexus, or inferior petrosal or transverse sinus.

The small variable occipital sinus lies in the midline at the attachment of the falx cerebelli, and it extends from the foramen magnum to drain upward into the torcular Herophili. Alternatively, with variant anatomy, the occipital sinus may drain toward the foramen magnum or into the jugular or suboccipital veins.

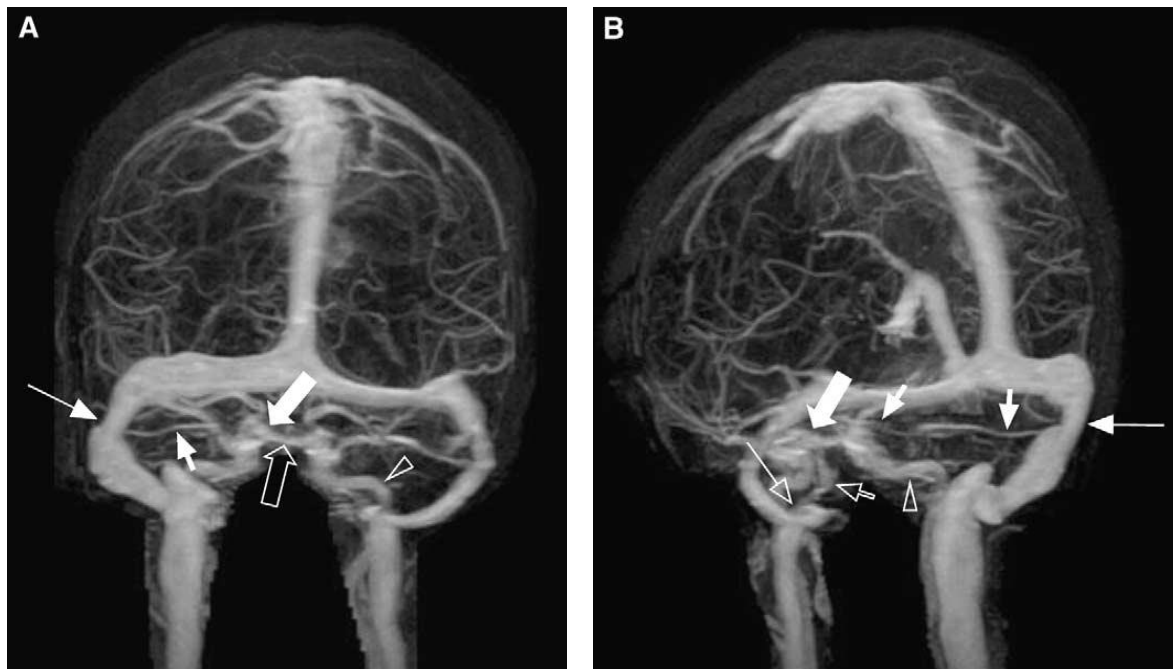


**FIG 4 -** Post segmentation MR venographic MIP images in (A) antero-posterior and (B) left anterior oblique projections demonstrate cavernous sinus relationships. Although partially obscured by basilar and cavernous carotid artery segments (open arrowheads) on these static images, the cavernous sinus (large arrow) can be seen to communicate across midline to its opposite cavernous sinus via the intercavernous sinus (open large arrow). The superior petrosal sinus (short arrows) drains posterolaterally from the cavernous sinus into the transverse sinus (long arrow), whereas the inferior petrosal sinus (open short arrows) opens more inferiorly into the jugular bulb (open long arrow). Delineation of these anatomic structures would improve during assessment of the routine 180 rotational MIP dataset

## **INFRATENTORIAL VEINS**

The veins of the brainstem form a superficial venous plexus deep to the arteries.

Veins of the medulla oblongata drain into the veins of the spinal cord or the adjacent dural venous sinuses, or the adjacent dural venous sinuses, or into variable radicular veins which accompany the last four cranial nerves to either the inferior petrosal or occipital sinuses, or to the superior bulb of the jugular vein.

Anterior and posterior median medullary veins may run along the anterior median fissure and posterior median sulcus, to become continuous with the spinal veins in corresponding positions.

Pontine veins, which may include a median vein and a lateral vein on each side, drain into the basal vein, cerebellar veins, the petrosal sinuses, transverse sinus or the venous plexus of the foramen ovale. Veins of the midbrain join the great cerebral vein or basal vein.

The veins of the cerebellum drain mainly into the sinuses adjacent to them or, from the superior surface, into the great cerebral vein.

The cerebellar veins course either run anteromedially across the superior vermis to the straight sinus or great cerebral vein, or they run laterally to the transverse and superior petrosal sinuses.

Inferior cerebellar veins include a small median vessel that runs backwards on the inferior vermis to enter the straight or sigmoid sinus. Laterally coursing vessels join the inferior petrosal and occipital sinuses.

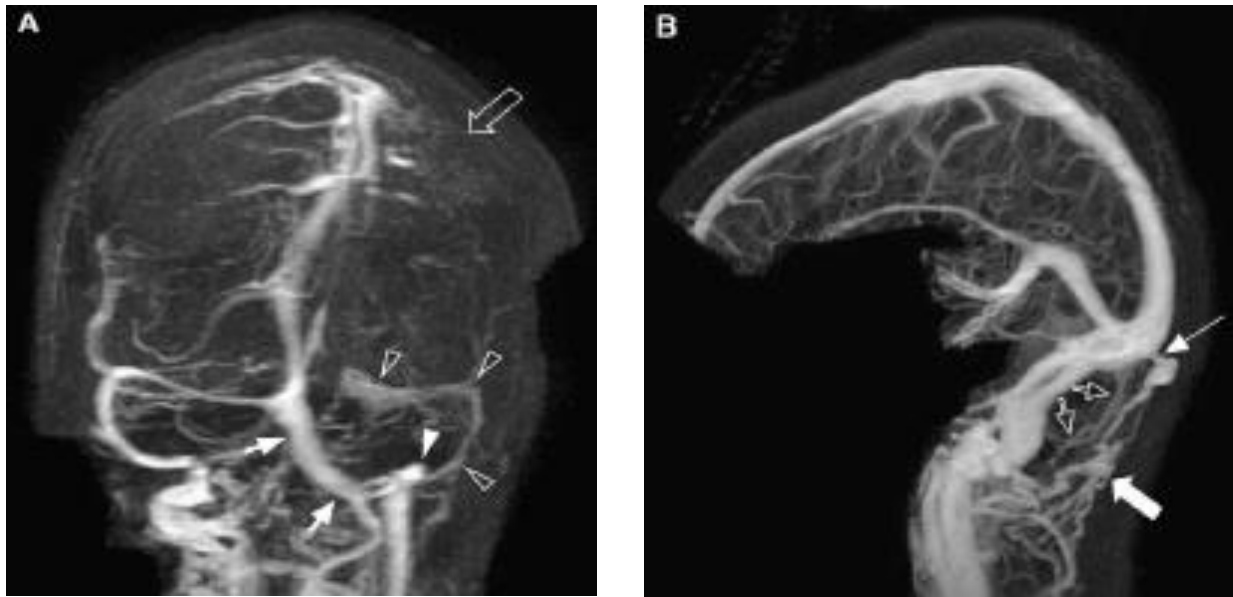


**FIG 5** - Two different patients in whom Intratentorial venous structures are noted on (A) antero-posterior and (B) Sagittal post segmentation MR venographic MIP images. (A) The midline occipital sinus (short arrows) drains from the torcular Herophili into the left jugular fossa (arrowhead), although minimal flow is still identified within the hypoplastic left transverse and sigmoid sinuses (open arrowheads). (B) The paired inferior vermian veins (open short arrows) course posterosuperiorly and usually open into the tentorial sinus. Also, note an occipital transcalvarial emissary vein (long arrow) and suboccipital venous plexus (large arrow).

## **ETIOLOGY, CLINICAL PRESENTATION, PATHOGENESIS AND DIAGNOSIS OF CVT**

Table 1: Risk factors for cerebral venous thrombosis<sup>23</sup>

<b>RISK FACTOR</b>	<b>DESCRIPTION</b>
Infection	Para nasal sinusitis Intracranial infection: abscess, meningitis
Trauma	Head trauma
	Neurosurgical interventions
	Internal jugular catheter
Medical/ Surgical conditions	Dehydration
	Pregnancy and puerperium
	Coagulation disorders : factor V Leiden (activated protein C resistance), protein C deficiency, protein S deficiency, antithrombin III deficiency, hyperhomocysteinemia, antiphospholipid syndrome
	Hematologic disorders: polycythemia, sickle cell disease, thrombotic thrombocytopenic purpura, Polycythemia, Paroxysmal nocturnal hemoglobinuria
	Malignancies, inflammatory bowel disease, Nephrotic syndrome, dehydration, liver cirrhosis, collagen vascular diseases, including systemic lupus erythematosus, Wegener granulomatosis and Behcet syndrome
	Previous surgical procedures
Medication	Oral contraceptives, hormone replacement therapy, L-asparaginase, aminocaproic acid, corticosteroids

## ETIOLOGY

The etiology of CVT is multifactorial and may involve one or more mechanisms<sup>24</sup>. Tissue damage and stasis (eg, trauma, surgery, and immobilization), hematologic disorders (eg, protein C, S deficiencies, increased resistance to activated protein C), malignancies, collagen vascular disease (eg: systemic lupus erythematosus, Behcet syndrome), pregnancy, and some medications (eg: oral contraceptives, hormone replacement therapy, and corticosteroids) have been reported to be predisposing factors for CVT (Table 1).

Despite multiple known risk factors, approximately 20% of patients with CVT do not have any known risk factors. In neonates, acute systemic illness, such as shock or dehydration, may be the cause. Frequent causes in older children include local infection, such as otitis media, mastoiditis, and coagulopathy. In adults, intrinsic or acquired coagulopathies become the most important factors, contributing to as many as 70% of cases. Infection contributes to less than 10% of cases in adults. In women of childbearing age, oral contraceptive use and pregnancy are strong risk factors<sup>25</sup>.

The main risk factors for deep venous cerebral thrombosis include oral contraception, postpartum, trauma, pregnancies, Crohn's disease, sickle cell disease, tumor, protein S deficiency, inflammation, paroxysmal nocturnal haemoglobinuria, diabetes mellitus, and nephrotic syndrome<sup>26</sup>.



Cerebral venous thrombosis (CVT) is responsible for 1–2% of all strokes in adults and affect all age groups. They estimated annual incidence of 3–4 cases per million people and a mortality rate of 8%. Isolated cortical venous thrombosis (ICoVT) (ie, without sinus involvement) appears extremely rare and has been mainly reported as isolated case reports or in small series<sup>27</sup>. Multiple locations of thrombosis, particularly in the contiguous transverse and sigmoid sinuses, are found in as many as 90% of patients.

The deep cerebral veins are involved in approximately 10% of patients. Cortical venous involvement is seen in 6% of patients but is likely to be underreported when the dominant imaging finding is dural sinus involvement<sup>28</sup>.

## **CLINICAL PRESENTATION**

The clinical presentation of CVT is variable but often includes headache and seizures (Table 2). In addition, the clinical presentation of CVT is closely related to the location and the extent of the thrombosis (cortical versus dural sinus, superficial versus deep). The clinical sequelae of CVT are related to the temporal evolution of the disease, the patient's venous anatomy, and the effectiveness of collateral venous pathways.

The most frequently occurring symptoms and signs of CVT are headaches, vomiting, and papilledema, reflecting increased cerebral venous pressure.

Although the symptoms are nonspecific, papilledema should prompt neuroimaging and CVT should be considered in the differential diagnosis. Patients may go on to develop seizures, decreased level of consciousness, or focal neurologic deficit. This progression of clinical signs and symptoms justifies neuroimaging on an emergency basis, and CVT is a diagnosis that must be ruled out.

**Table 2 - Clinical presentation of CVT**

Clinical presentation of CVT is dependent on the location and extent of the thrombosis.

SYMPTOMS	Headache
	Double vision
	Blurred vision
	Altered consciousness
	Nausea, vomiting
	Seizures
SIGNS	Papilledema
	Focal neurologic deficit
	Cranial nerve palsies
	Nystagmus

Focal neurologic deficit may develop, depending on the area involved. Hemiparesis may occur, and in some cases of sagittal sinus thrombosis, weakness may develop in the lower extremity.

This also may occur as bilateral lower extremity involvement. Aphasia, ataxia, dizziness, chorea, and hemianopia all have been described<sup>29</sup>.

Cranial nerve syndromes are seen with venous sinus thrombosis. These include the following:

- Vestibular neuronopathy
- Pulsatile tinnitus

- Unilateral deafness
- Double vision
- Facial weakness
- Obscuration of vision

The prognosis of CVT has traditionally been considered poor. Two prospective reports found that 41% of patients had a poor outcome, defined as death or a Barthel index score of less than 15%. Recent reports, however, have shown mortality rates to be less than 10%. for CVT in pregnancy and in the puerperium has a more acute onset and a better prognosis (9% versus 33%) compared with thrombosis from other causes.

The venous sinus is a cavity formed between the endosteal and meningeal layers of the dura. The sinuses are connected by channels to large cortical veins and together make up the venous system that allows blood to drain from the cranium. Thrombus formation within a venous sinus can create a partial or complete blockage and localized congestion within the venous system and the brain; both are secondary to decreased venous outflow (Chow et al., 2000; Ekseth et al., 1998). Exacerbation of venous congestion causes increased intracranial pressure, massive ischemia, and infarction of cerebral tissue (Ekseth et al.). Hemorrhagic conversion can occur in larger infarctions

Venous thrombosis has a nonspecific presentation and therefore it is important to recognize subtle imaging findings and indirect signs that may indicate the presence of thrombosis. Although these findings are often present on initial scans, they are frequently detected only in retrospect. In addition, the imaging findings are often subtle. Underdiagnosis or misdiagnosis of cerebral venous thrombosis can lead to severe consequences, including hemorrhagic infarction and death<sup>30</sup>.

The pathogenesis of CVT is complex and remains poorly understood. In 20–35% of cases, the cause remains unknown; therefore, one should remain suspicious, even in the absence of known risk factors<sup>31</sup>.

## **PATHOPHYSIOLOGY OF CVT**

Venous obstruction results in increased venous pressure, increased intracranial pressure, decreased perfusion pressure and decreased cerebral blood flow.



Increased venous pressure may result in vasogenic edema from breakdown of the blood brain barrier and extravasation of fluid into the extracellular space.



Blood also may extravasate into the extracellular space.



Severely decreased blood flow also may result in cytotoxic edema associated with infarction.



Parenchymal findings on imaging correlate with degree of venous pressure elevation with mild to moderate pressure elevations; there is parenchymal swelling with sulcal effacement but without signal abnormality. As pressure elevations become more severe, there is increasing edema and development of intraparenchymal hemorrhage in upto 40 % of patients who have CVT.

Acute arterial ischemia causes a sudden drop of sodium – potassium ATPase pump leading to intracellular migration of water and subsequent cytotoxic edema, whereas in a case of cerebral venous thrombosis congestion leads to vasogenic edema initially and at a later stage cytotoxic edema.

## **DIAGNOSIS OF CVT**

<b>When to think of venous thrombosis</b>	
<b>Direct sign of thrombus</b>	Dense clot sign Cord sign Empty delta Loss of normal flow void on MR
<b>Venous infarction</b>	Bilateral - <i>parasagittal bithalamic</i> Temporal lobe infarction Cortical edema or hemorrhage Peripheral lobar hemorrhage
<b>Clinically</b>	Seizures Headache Loss of consciousness

The prospective clinical diagnosis of cerebral venous thrombosis is difficult because of a wide spectrum of clinical manifestations; the diagnosis is typically made on the basis of imaging studies. The most commonly described symptoms are headache, seizures, mental obtundation, and focal motor or sensory deficits<sup>32</sup>.

### **Direct signs of a thrombus**

#### **Dense clot sign**

Direct visualization of a clot in the cerebral veins on a non-enhanced CT scan is known as the dense clot sign. It is seen in only one third of cases.

Normally veins are slightly denser than brain tissue and in some cases it is difficult to say whether the vein is normal or too dense. In these cases a contrast enhanced scan is necessary to solve this problem.

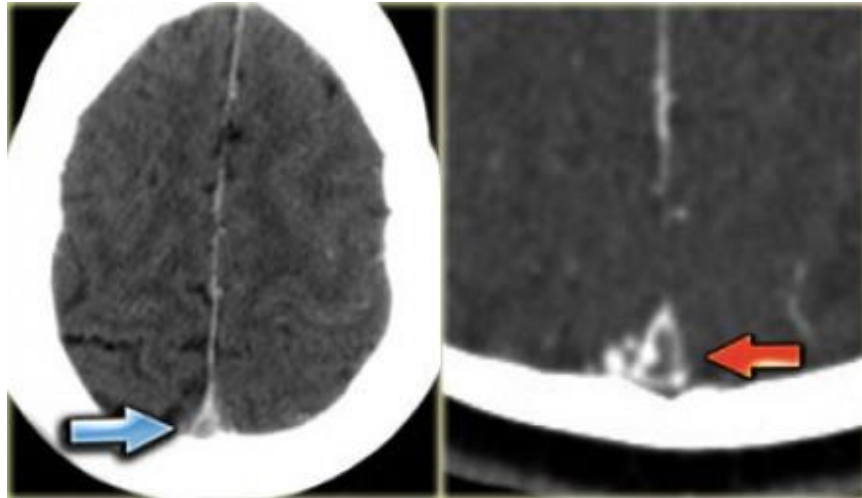
Visualization of a thrombosed cortical vein that is seen as a linear or cord-like density is also known as the cord sign<sup>33</sup>.

## **Empty delta sign**

The empty delta sign is a finding that is seen on a contrast enhanced CT (CECT) and was first described in thrombosis of the superior sagittal sinus.

The sign consists of a triangular area of enhancement with a relatively low-attenuating center, which is the thrombosed sinus. The likely explanation is enhancement of the rich dural venous collateral circulation surrounding the thrombosed sinus, producing the central region of low attenuation as shown in the figure below.

This sign may be absent after two months due to recanalization within the thrombus<sup>34</sup>.



Empty delta sign: Note the triangular area of enhancement with a relatively low-attenuating center, which is the thrombosed sinus

## Absence of normal flow void on MR

On spin-echo images patent cerebral veins usually will demonstrate low signal intensity due to flow void. Flow voids are best seen on T2-weighted and FLAIR images, but can sometimes also be seen on T1-weighted images.

A thrombus will manifest as absence of flow void. Although this is not a completely reliable sign, it is often one of the first things that make the possibility of venous thrombosis. The next step has to be a contrast enhanced study

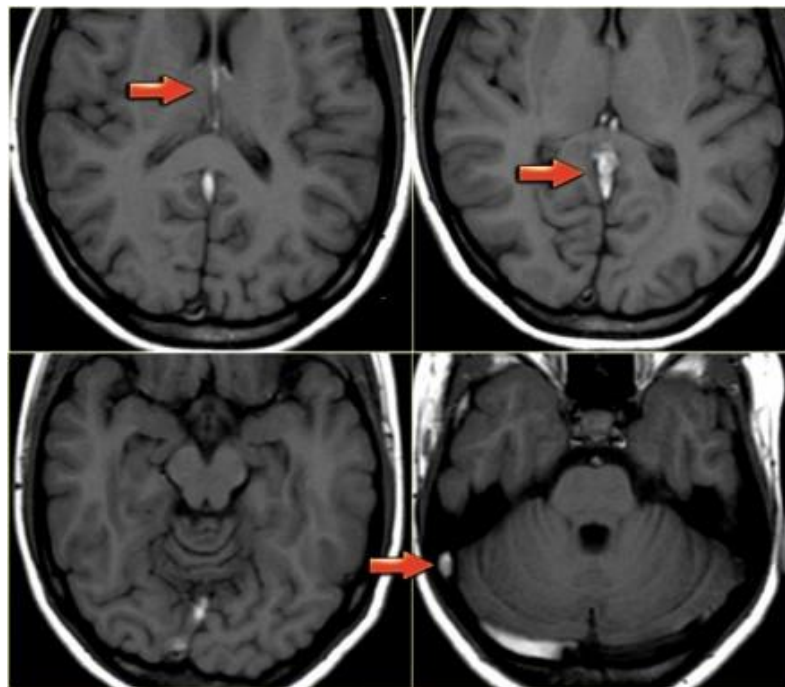


FIG-6 The images on the left show abnormal high signal on the T1-weighted images due to thrombosis. The thrombosis extends from the deep cerebral veins and straight sinus to the transverse and sigmoid sinus on the right. Notice the normal flow void in the left transverse sinus on the right lower image.

## Venous infarction

Venous thrombosis leads to a high venous pressure which first results in vasogenic edema in the white matter of the affected area. When the process continues it may lead to infarction and development of cytotoxic edema after the vasogenic edema. This is unlike in an arterial infarction in which there is only cytotoxic edema and no vasogenic edema. Due to the high venous pressure hemorrhage is seen more frequently in venous infarction compared to arterial infarction. Since many veins are midline structures, venous infarcts are often bilateral. This is seen in thrombosis of the superior sagittal sinus, straight sinus and the internal cerebral veins<sup>35</sup>.

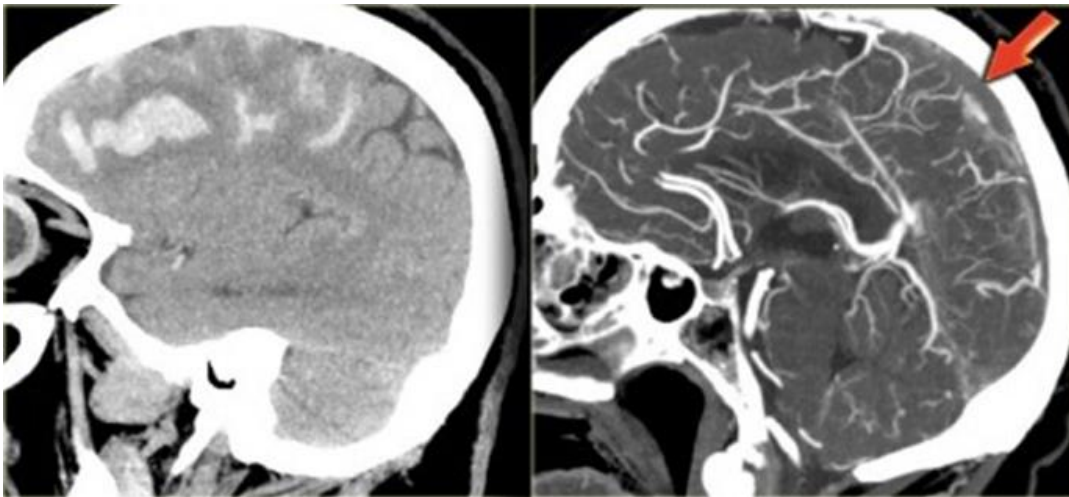


FIG-7 On the left reconstructed sagittal CT-images in a patient with bilateral parasagittal hemorrhage due to thrombosis of the superior sagittal sinus. The contrast enhanced image indicates the filling defect caused by the thrombus.



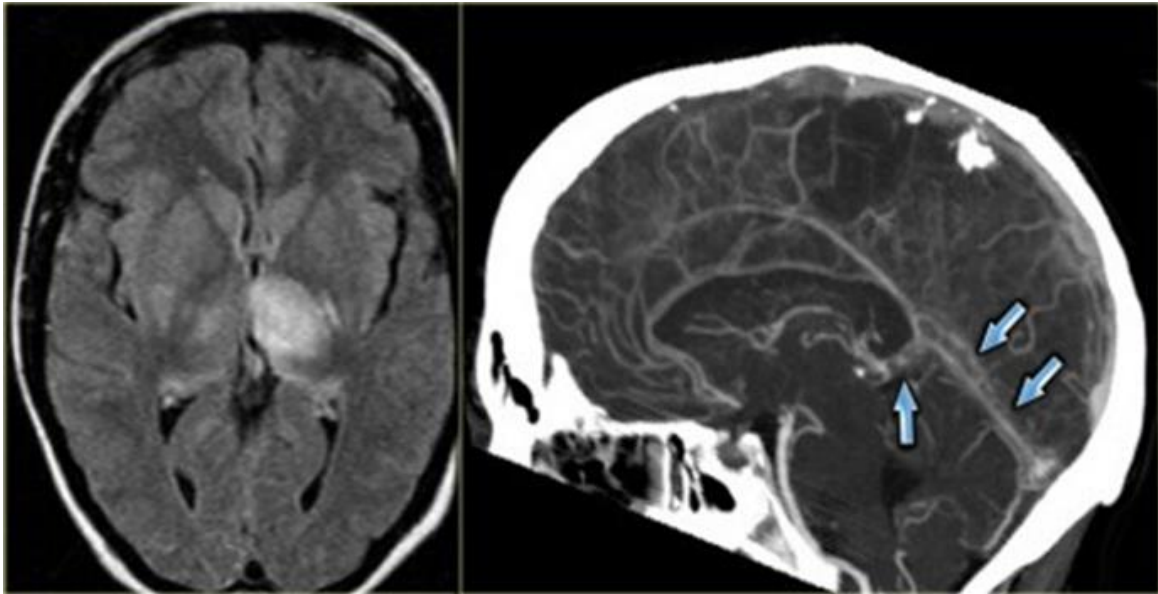


FIG-8 On the left a FLAIR image demonstrating high signal in the left thalamus. there is also high signal in the basal ganglia on the right. These bilateral findings should raise the suspicion of deep cerebral venous thrombosis A sagittal CT reconstruction demonstrates a filling defect in the straight sinus and the vein of Galen (arrows).

## Computed tomography

CT is the initial modality of investigation of choice for most neurological conditions. Its widespread availability, comparatively shorter scan times and lower cost. It is reported that in the acute phase of CVT, almost 38% of CT scans are normal. Thrombus is visible on non-enhanced CT as a high-attenuation lesion in the venous channel, producing dense triangle or cord sign represents an intravascular acute blood clot. This sign is reported in 20% of patients and takes approximately 1–2 weeks to disappear.

However, similarly increased attenuation of the cerebral venous sinuses may also represent polycythemia, dehydration, a subjacent subarachnoid or subdural hemorrhage and nonmyelinated brain in neonates makes sinuses appear unusually attenuating<sup>36</sup>. Increased attenuation in the sinus may be the only finding suggestive of sinus thrombosis on unenhanced CT images, and

patients with this sign should be further evaluated with contrast-enhanced CT, MR imaging, or both, in the proper clinical scenario.

## CT-venography

CT-venography (CTV) is a simple and straight forward technique to demonstrate venous thrombosis. In the early stage there is non-enhancement of the thrombosed vein and in a later stage there is non-enhancement of the thrombus with surrounding enhancement known as empty delta sign, as discussed before. CT-venography virtually has no pitfalls.

First, two-dimensional (2D) MPR images are used to visualize dural venous sinuses and cerebral veins, with adequate window level and width. Second, 2D maximum intensity projection (MIP) series are created and saved. Optional reformations include 3D MIP and volume rendering display algorithms. CT and CTV remains a rapid screening modality for early diagnosis of CVT in the emergency setting<sup>37</sup>. In patients with unenhanced CT findings suggestive of venous thrombosis, Multidetector Computed Tomography (MDCT) venography can be performed without delay to confirm the diagnosis and to start appropriate therapy immediately.

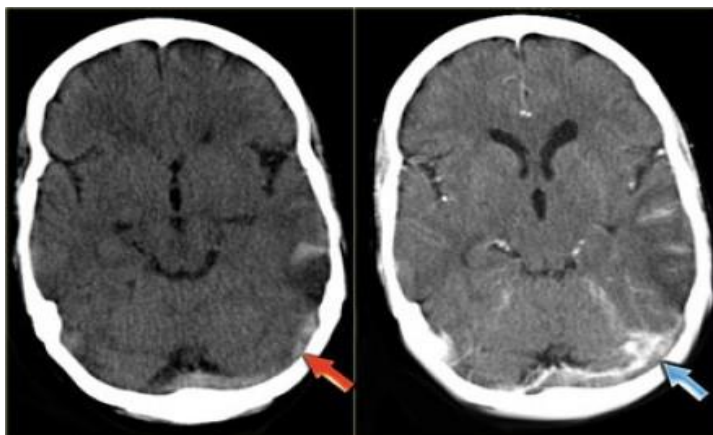


FIG9 On the left image there is an infarction in the area of the vein of Labbe. On the non-enhanced images the dense thrombus within the transverse sinus and the hemorrhage in the infarcted area is demonstrated. On the enhanced images a filling defect can be seen in the transverse sinus.

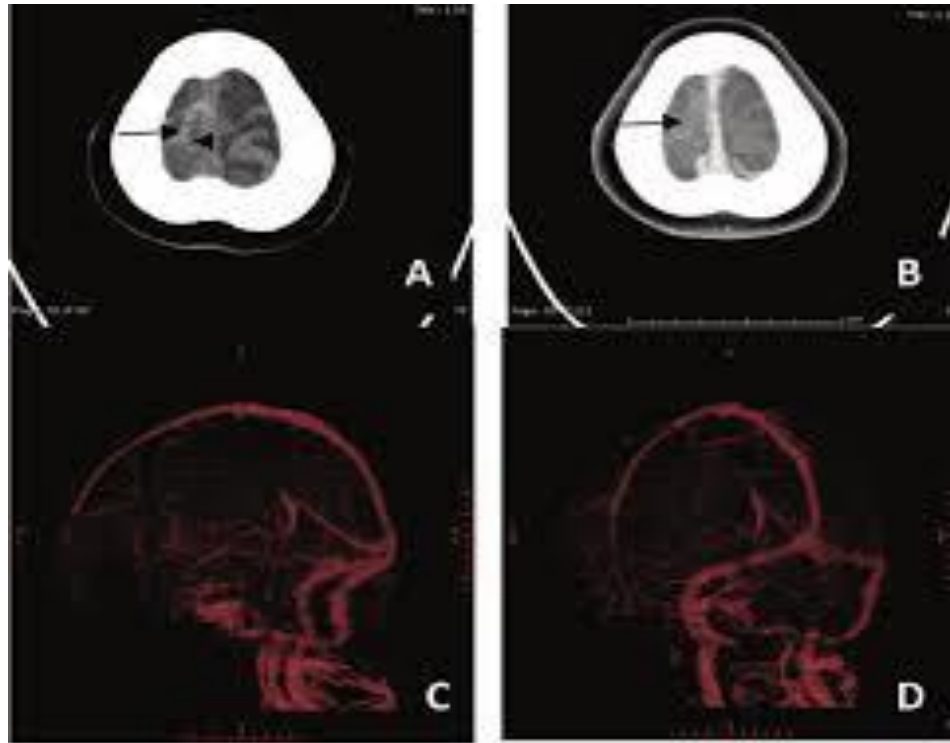


FIG 10 Axial computed-tomography scan demonstrates A,B) intraluminal hyperdensity of clot at right sided of superior sagittal sinus wall, cortical veins of right frontal regions (cord sign, arrow). CT venography showed (C,D) no contrast filled in thrombosed cortical vein in right frontal region. The dural venous sinus is well opacified by contrast medium.

## MRI

On MRI, venous thrombus may be directly visualized. On conventional MRI sequences, patent dural sinuses are often seen as a flow void. This is particularly well seen when the imaging plane is orthogonal to the blood flow direction (e.g., coronal images are best for visualization of the superior sagittal, transverse, and sigmoid sinuses). The effect of a flow void may be reduced in a plane parallel to the dural sinus, although such an imaging plane often offers a better depiction of the complete extent of thrombosis in the dural sinus. The thrombus may manifest as absence of a flow void, which is often best seen on FLAIR images and T2-weighted spin-echo images<sup>33</sup>.

On T1-weighted images, thrombus with methemoglobin is seen as hyperintensity. On T2\*-weighted gradient-echo images, exaggerated signal loss is often seen because of the increased susceptibility effect of deoxyhemoglobin, methemoglobin, or hemosiderin.

Indirect evidence of venous thrombosis is often secondary to parenchymal change as a result of venous occlusion. This is similar to the findings on CT, including brain swelling and hemorrhagic or nonhemorrhagic infarction. Conventional MRI sequences often provide sufficient information to raise the suspicion or to make a diagnosis of CVT. The diagnosis can then be further confirmed on MR venography or CT venography

Magnetic resonance imaging (MRI) with MR venography has become the investigation of choice in diagnosis of CVT. MRI is more sensitive in picking up the thrombus, and demonstrates age dependant signal characteristics. One of the most important findings on MRI is abnormal signal intensity within the venous structure, indicating altered flow and thrombus formation<sup>38</sup>.

There has been recent interest in evaluating the appearance of intraluminal venous thrombi on DWI. Signal hyperintensity in thrombosed sinuses on diffusion weighted images, with corresponding diminishment in the mean apparent diffusion coefficient (ADC) values, has been described in 41% of patients with sinus thrombosis. The duration of clinical symptoms was longer and complete recanalization was less frequent in patients with restricted diffusion in the thrombus

Thalamic edema is the imaging hallmark of deep venous occlusion (e.g. internal cerebral vein, vein of Galen, or straight sinus), demonstrating hyperintensity on T2 and FLAIR weighted images. It may extend into the caudate regions and deep white matter. Hemorrhage is noted in 19% of patients and typically is located in the thalami. Unilateral thalamic edema may occur but is rare. The lack of flow-void in the deep venous system is very suggestive for a venous thrombosis. At present, MR has become the method of choice for the diagnosis and follow-up of deep venous thrombosis because of its sensitivity to visualize thrombus,<sup>39</sup>.

Isolated cortical venous thrombosis is a relatively rare entity. It is particularly difficult to diagnose by using only T1WI, T2WI, and MRV imaging for different reasons (e.g. cortical veins are extremely variable in number, size, and location; occluded small veins at the cortical level are difficult to identify by using these MRI; only the occlusion of the largest veins is detectable on MRV). Typical parenchymal findings are areas of focal cortical edema or hemorrhage, which may be nonspecific. The hyperintense vein sign is seen on MRI. Blooming artifacts within the thrombosed veins can be a very useful adjunct finding on GRE images.

## **DIFFUSION-WEIGHTED IMAGING IN CVT**

Venous infarction differs from arterial infarction in that acute venous occlusion is thought to result in acute vasogenic edema because of increased capillary filtration pressure and extravasation of fluid. Inadequate perfusion pressure may also cause energy failure and cytotoxic edema. Therefore, a combination of both vasogenic and cytotoxic edema may coexist in the acute phase of CVT. Early hemorrhagic transformation may also complicate interpretation of MRI in these patients. Because of these differences in pathophysiologic characteristics, DWI has proved helpful in the differentiation of venous from arterial infarction and in the prediction of tissue outcome.

Diffusion-weighted imaging (DWI) is an MRI sequence, first developed by Le Bihan et al, that is sensitive to the diffusion of water protons. The application of DWI in diagnosing arterial stroke is well established and has been demonstrated by numerous experimental and clinical studies.

DWI is based on the random motion or diffusion of water molecules, and can provide apparent diffusion coefficients (ADC) that indicate whether affected cerebral edema is of Cytotoxic or vasogenic edema, since the conventional MR imaging cannot distinguish between Cytotoxic and vasogenic edema.

T2 W hyperintense lesions may have decreased diffusion, elevated diffusion, or a mixed pattern. Lesions with elevated diffusion represent vasogenic edema. Vasogenic edema is hyperintense on ADC maps and hypointense on exponential images.

Lesions with decreased diffusion are believed to represent cytotoxic edema. Cytotoxic edema is hypointense in ADC maps and hyperintense on exponential images. Unlike arterial stroke, some of these lesions resolve and some persist. Resolution of lesions with low ADC values may be related to better drainage of blood through collateral pathways in some patients

The diffusion of water protons can be quantitated by a parameter known as apparent diffusion coefficient (ADC). Brain regions with restricted diffusion due to cytotoxic edema appear dark on ADC maps. Chronic brain infarcts with high cerebrospinal fluid content appear bright on ADC maps. Similarly, ADC maps depict regions of vasogenic edema as a bright signal owing to increased extracellular water content in the edematous regions. The combination of DWI and ADC can therefore discriminate between acute and chronic ischemia, and between vasogenic and cytotoxic edema. This represents a considerable advance over conventional MRI techniques such as fluid – attenuated inversion recovery (FLAIR) and T2W, in which acute or chronic ischemia and vasogenic or Cytotoxic edema all appear bright.

Diffusion-weighted imaging in cases of cerebral venous thrombosis (CVT), the apparent diffusion coefficient (ADC) was shown to be decreased, normal or increased. Moreover, the prognostic value of the ADC in acute venous stroke is still debated, although it has been recently suggested that diffusion-weighted imaging could noninvasively help in selecting those patients with CVT who would benefit from more aggressive treatments<sup>40</sup>.

Keller et al reported the finding in a case of deep cerebral venous thrombosis with extensive hyperintensities in the basal ganglia on T2 weighted images and hypointensities on diffusion-weighted images, with increased ADC values ( $1.1$  to  $1.6 \times 10^{-3} \text{ mm}^2/\text{S}$ ). These findings were explained as being the result of vasogenic edema. The patient was treated with IV heparin and had total clinical recovery; no parenchymal defects were revealed during follow up MR examinations<sup>41</sup>.

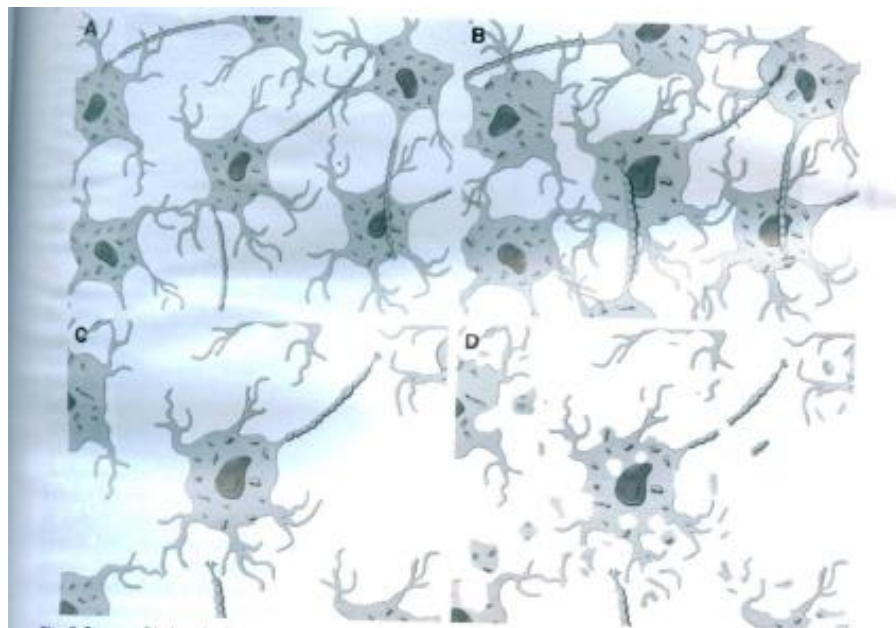


**FIG11** - Stages of ischemic damage to brain tissue. A) Normal gray matter. B) Cytotoxic edema. Within minutes after onset of ischemia, failure of energy dependent membrane ion pumps cause an accumulation of ions in the intracellular space. Water follows by osmosis, resulting in cellular swelling. This process is associated with a decrease in ADC and accounts for DWI's superior sensitivity in the detection of acute infarcts. C) Vasogenic edema. Release of inflammatory mediators results in efflux of new water from the vasculature, which is associated with an increase in ADC. Vasogenic edema becomes evident on MR imaging within approximately 6 hours after stroke onset and peaks approximately 3 to 5 days thereafter. D) Cellular breakdown. During the ensuing weeks, months, and years, breakdown of cellular membranes and gradual phagocytosis of necrotic debris further remove restrictions on water diffusion, resulting in further increase in ADC.



## **SUSCEPTIBILITY WEIGHTED IMAGING IN CVT**

Susceptibility weighted imaging (SWI) is an magnetic resonance (MR) technique that is exquisitely sensitive to paramagnetic substances, such as deoxygenated blood, blood products, iron, and calcium. This Sequence is a high-resolution three-dimensional (3D), fully velocity-compensated, gradient echo (GRE) sequence, wherein the phase images are used to create a phase mask after unwrapping and high pass filtering, which is then multiplied with the magnitude images to enhance the conspicuity of small veins and other paramagnetic substances. The clinical utility of this technique has been described in variety of neurological disorders, such as trauma, tumours, vascular malformations, multiple sclerosis, venous thrombosis, and stroke.

The local magnetic heterogeneity induced by paramagnetic, diamagnetic, and ferromagnetic substances can result in overall signal loss in GRE images. The susceptibility effect is highest in GRE techniques at long echo times and higher field strengths. The high spatial resolution 3D fast low angle shot (FLASH) technique is used, as this is extremely sensitive to susceptibility effects. All MR image data have magnitude and phase information, though the phase information is not routinely utilized for image formation.

This phase information can be easily obtained with all imaging sequences and this requires no additional imaging time. Deoxygenated haemoglobin and other paramagnetic substances produce a positive shift, whereas diamagnetic substances, such as calcium, induce a shift in the opposite direction. The inhomogeneities arising from the static magnetic fields are usually in the low frequency range and are removed using homodyne demodulation reference, which is a common and easily implemented technique.

High-pass filtering is then performed by subtracting a low-pass filtered, unwrapped phase image from the original unwrapped phase image.. These are then multiplied with magnitude images to enhance the visualization of small veins or microbleeds. These images are further processed with minimum intensity projections (MIP) to obtain nine to 12 thick MIP slabs<sup>42</sup>.

Cerebral venous thrombosis can present with non-specific clinical manifestations unrecognizable to the physician, and its diagnosis remains extremely important as the consequences of mistreatment can be devastating. T2\*W sequences have high sensitivity in detecting cerebral venous thrombosis, especially in cortical vein thrombosis .However, the clot can appear hypointense on T2\*W images depending on the proportion of deoxyhaemoglobin, and this may be confused with flow artefacts or magnetic susceptibility effects from adjacent bone or air sinuses and hence cannot be used in isolation. Analysis of both phase and magnitude images can be helpful to differentiate a dilated from thrombosed vein. Asymmetrical prominent veins over the cerebral convexities observed due to the high concentrations deoxyhaemoglobin secondary to venous stasis may sometimes be the only clue to the unsuspected thrombosis. Diffuse symmetrical paucity or prominence of veins is related to the concentration of oxyhaemoglobin within the veins.

SWI provides a unique contrast, similar to blood oxygen level dependent (BOLD) imaging, which is widely used in functional imaging. When there is hypoperfusion of any region of the brain due to deficient arterial supply, it promotes focal vasodilatation. This causes relative

slowing of the circulation and increased extraction of oxygen from the blood in the ischemic region. This causes a focal increase in the concentration of deoxyhemoglobin in the venous blood. As deoxyhemoglobin is paramagnetic, this can be detected by SWI. Therefore, venous vessels in the ischemic region appear hypointense and prominent<sup>43-45</sup>.

## **MR VENOGRAM IN CVT**

The use of cerebral MR venography is increasing in frequency as a noninvasive means of evaluating the intracranial venous system. This technique is particularly useful in the diagnosis of venous sinus thrombosis, which at times can be difficult.

Dural venous sinus thrombosis, seen in a number of conditions, including dehydration, hypercoagulable states, infection, tumor invasion, and in conjunction with oral contraception, may be a cause of neurologic deterioration. This diagnosis has traditionally been made during the venous phase of conventional catheter angiography, which has been considered the standard of reference . This is however, an invasive procedure with well-known associated risks . Recent reports have suggested that perhaps MR imaging and MR venography may be able to replace conventional angiography in the diagnosis of dural venous sinus thrombosis<sup>46</sup>.

The MR-techniques that are used for the diagnosis of cerebral venous thrombosis are:Time-of-flight (TOF), phase-contrast angiography (PCA) and contrast-enhanced MR-venography:

Time-of-Flight angiography is based on the phenomenon of flow-related enhancement of spins entering into an imaging slice. As a result of being unsaturated, these spins give more signal than surrounding saturated spins.

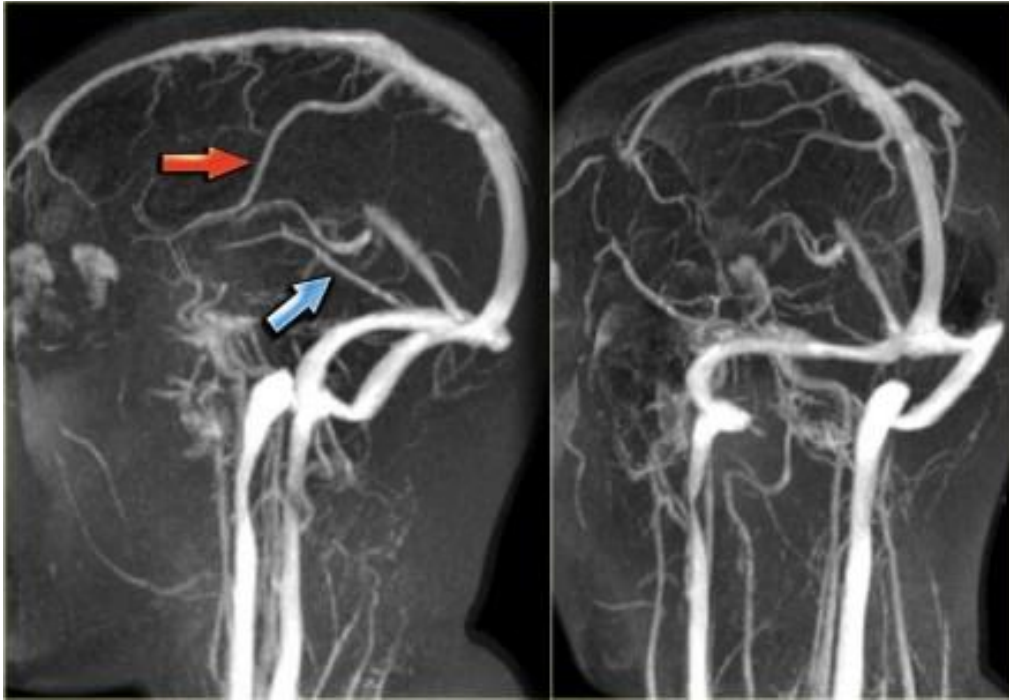
Phase-contrast angiography uses the principle that spins in blood that is moving in the same direction as a magnetic field gradient develop phase shift that is proportional to the velocity of the spins

This information can be used to determine the velocity of the spins. This image can be subtracted from the image that is acquired without the velocity encoding gradients, to obtain an angiogram.

Contrast-enhanced MR-venography uses the T1-shortening of Gadolinium. It is similar to contrast-enhanced CT-venography

Whereas TOF techniques rely mainly on flow related enhancement for producing vascular images, phase-contrast MR angiography uses velocity induced phase shifts imparted upon the moving spins to distinguish flowing blood from the surrounding stationary tissue. Although excellent background suppression is a major advantage, and quantitative determination of blood velocities may be possible, phase-contrast MR angiography may require long imaging times and a prior estimate of blood flow velocity; it may also be more sensitive to signal loss due to turbulence or intravoxel dephasing.

After acquisition of the stack of contiguous 2D-TOF slices, the image volume is subjected to the MIP ray tracing algorithm to present the MR venogram in a format similar to that generated by conventional angiography<sup>47, 48</sup>.



Lateral and oblique MIP image from a normal contrast-enhanced MR venography.  
Notice the prominent vein of Trolard and vein of Labbe(arrows)

The diagnosis of cerebral venous thrombosis is often difficult both clinically and radiologically. Until now, there is no method available to predict if brain lesions, detected clinically and using conventional MR imaging methods, may lead to full recovery, as expected in arterial infarcts and even a hematoma<sup>49</sup>.

Cerebral venous thrombosis (CVT) differs from arterial infarction in several ways. First, the clinical presentation is variable, may range from subacute headache, raised intracranial pressure to severe multifocal deficits, seizure, and coma. Accurate diagnosis is difficult but important because effective therapies, including anticoagulation and possibly intrasinus thrombolysis, are available. In fact, patients with CVT often make dramatic recoveries after anticoagulation, even when treatment is delayed. For this reason, accurate diagnosis is important even beyond the hyperacute period<sup>50</sup>.

Venous infarction also differs from arterial infarction in that acute venous occlusion is thought to result in acute vasogenic edema because of increased capillary filtration pressure and extravasation of fluid<sup>51</sup>. Inadequate perfusion pressure may also cause energy failure and cytotoxic edema. Therefore, a combination of both vasogenic and cytotoxic edema may coexist in the acute phase of CVT. Early hemorrhagic transformation may also complicate interpretation of MRI in these patients, because of these differences in pathophysiologic characteristics, DWI has proved helpful in the differentiation of venous from arterial infarction and in the prediction of tissue outcome.

There may be a wide range of signs and symptoms at presentation, so in almost any cerebral syndrome, CVT could be considered. However certain clinical features provide clue to the presence of CVT. Since growth of thrombus is usually slow, and venous collateralization is extensive, the symptoms typically evolve over days or weeks, although the onset may be acute. The severity of symptoms depends on chronicity of development and on the vessels involved. Headache is a key presenting feature and since this may be associated with papilledema, it may

be confused with benign intracranial hypertension. Seizures and focal deficits resulting from infarction or venous edema may be present

In the setting of acute ischemia, cellular energy failure leads to cytotoxic edema, characterized by a shift of water molecules from the extracellular to the intracellular space. The resulting restricted diffusion of these water molecules is displayed as a bright signal on DWI. In the clinical setting, DWI has detected acute brain ischemia within 39 minutes of onset. In contrast to acute ischemic lesions, chronic brain infarcts generally do not appear bright on DWI. Because cerebrospinal fluid that has unrestricted water proton diffusion, replaces infarcted tissue. However, there is a T2 contribution to signal intensity on DWI, which occasionally results in a bright signal in chronic infarcts or other lesions ('T2 shine through').

The diffusion of water protons can be quantitated by a parameter known as apparent diffusion coefficient (ADC). Brain regions with restricted diffusion due to cytotoxic edema appear dark on ADC maps. Chronic brain infarcts with high cerebrospinal fluid content appear bright on ADC maps. Similarly, ADC maps depict regions of vasogenic edema as a bright signal owing to increased extracellular water content in the edematous regions. The combination of DWI and ADC can therefore discriminate between acute and chronic ischemia, and between vasogenic and cytotoxic edema. This represents a considerable advance over conventional MRI techniques such as fluid attenuated inversion recovery (FLAIR) and T2W, in which acute and chronic ischemia and vasogenic and cytotoxic edema all appear bright<sup>52</sup>.

The study by **Chu et al** describes 14 patients with confirmed CVT studied with DWI and ADC mapping at variable times from onset of symptoms. The authors were able to delineate three general patterns of MRI abnormality. The most common was heterogeneous signal intensity on DWI with normal or increased ADC values. This pattern most likely represents vasogenic edema in combination with cytotoxic edema. The ADC map was particularly useful for differentiating vasogenic from cytotoxic edema, both of which appear bright on conventional images.

In venous stroke, even large parenchymal changes can resolve completely independent from recanalisation of the thrombosed veins and sinuses. A plausible hypothesis is that venous infarcts largely consist of a persistent edema and that the lesion volume is influenced by the development of collateral veins. Restricted water diffusion suggesting cytotoxic edema is commonly found in subjects with acute cerebral venous infarction and decreases over time. This supports an important etiologic role for cytotoxic edema in the pathogenesis of cerebral venous infarction<sup>53</sup>.

**Marie-Germaine Bousseret et al in 2007**, conducted a study to derive high diagnostic value of susceptibility weighted imaging in CVT. In their study, MRV showed the presence of an occluded vein or sinus in 37/39 patients at the first MRI examination. The most important finding of this study is that a MSE (magnetic susceptibility effect) was detected at 90% sites of venous thrombosis at the first MRI investigation. The sensitivity of T2\*SW and T1-weighted spin echo image (T1SE) sequences to detect clot in the sinuses or veins was estimated at 90% and 71% between day 1 and day 3, which was much higher than that of T2SE, FLAIR or DWI during



the first week of clinical onset. The sensitivity of T2\*SW was stable in the first week. Thrombosed cortical veins, even in the absence of visible occlusion on magnetic resonance venography, were detected more frequently with T2\*SW (97%) and T1SE (78%) than with FLAIR or DWI (~40%). These data suggest that The T2\*SW sequence may be particularly useful during the acute phase of CVT when the sensitivity of the other sequences is incomplete and for the diagnosis of isolated cortical venous thrombosis<sup>54</sup>.

Magnetic resonance imaging, and recently MR venography, has increased the ability to detect CVT. MRI offers major advantage for the evaluation of patients suspected of dural sinus thrombosis because of its ability to visualize the thrombus, its sensitivity to flowing blood and being noninvasive and radiation free. MR was considered as the investigation of choice for the diagnosis of dural sinus thrombosis. However, complex signal intensity pattern of flowing blood on MR images has made it difficult to distinguish between thrombosis and flow-related enhancement. This difficulty has led to use of MR venography in the evaluation of CVT and other abnormalities of cerebral venous system. The technique of choice for diagnostic evaluation and follow up of dural sinus thrombosis is MR venography. The MR techniques that are used for the diagnosis of cerebral venous thrombosis are: Time-of-flight (TOF), phase-contrast angiography (PCA) and contrast-enhanced MR-venography. Contrast MR venography is considered more superior to TOF venography.

**Khaladkar SM et al** in 2014 did a retrospective case series analysis in patients of CVT on MRI. They concluded that MRI and MRV are efficacious in detecting cerebral venous sinus thrombosis and brain parenchymal abnormalities due to CVT. Deep venous system involvement

and isolated cortical vein thrombosis can be detected. These help in early detection and management of CVT to avoid neurological deficit. MRV is useful for demonstrating recanalization of thrombosed venous sinuses<sup>55</sup>.

**Boussier et al.** stated that thrombosis of deep cerebral venous system is rare and difficult to diagnose. In their study, the most common sinus involved was superior sagittal sinus with almost equal involvement of transverse sinus and sigmoid sinus. The deep venous system was involved in 17.5% patients and superficial venous system in 2.5% of cases. Commonest association was noticed between superior sagittal and transverse or sigmoid sinus.

**Greiner et al.** concluded that in veno-occlusive stroke, the superior sagittal sinus followed by transverse, sigmoid, and straight were generally involved<sup>56</sup>.

**D. Karthikeyan et al.** stated that headache is the most presenting and non-specific symptoms seen in 70-90% of CVT cases. Headache in most of the cases is unilateral. Focal neurological deficits such as hemiparesis, hemisensory disturbance, seizures, impairment of level of consciousness and papilledema occur in one-third to three-quarters of cases. The onset may be acute, subacute or insidious. Patients may present with symptoms that have evolved over days or weeks<sup>57</sup>.

Puerperium states are also associated with increased risk of CVT. Pregnancy induces a prothrombotic state that can be exacerbated by delivery trauma and dehydration associated with labour. CVT is more common in the third trimester and for six to eight weeks postpartum<sup>50</sup>. Approximately 2% of pregnancy-associated strokes are due to CVT.

CVT occurs more commonly in patients taking third generation OCPs. The mechanism by which hormonal stimulation increases the risk of venous thrombosis is unknown. Hormone therapy does impair protein-S activity and increases prothrombin levels in the blood leading to a hypercoagulable state. OCPs may also increase levels of fibrinogen and factors VII, VIII, and X thereby increasing a patient's risk of venous thrombosis<sup>58</sup>.

The risks of long-standing epilepsy and of CVT recurrence are low. In particular, no recurrence was observed in women who later became pregnant. In most cases, there is no need for long-term anticoagulant or anticonvulsant treatment. However, these are required on a case-by-case basis in the few patients who have recurrent thrombotic (cerebral or systemic) events or recurrent seizures<sup>59</sup>. In the absence of known thrombophilia, heparin treatment during further pregnancies is not required, but a short-term preventive treatment during the first 2 postpartum weeks is probably judicious.

## **TREATMENT**

**MEDICAL CARE:** Initial management revolves around the stabilizing the patient. Seizures should be treated with appropriate anticonvulsants. Specific therapy for CVT involves anticoagulation or thrombolytic therapy.

The current management for CVT is determined mostly on a case-by-case basis<sup>60</sup>. In general, anticoagulation using heparin has been used as a safe and clinically effective treatment method<sup>61</sup>. Recently, endovascular management, including direct thrombolysis with or without mechanical

thrombus extraction, has been advocated and has shown favorable outcomes<sup>62</sup>. These reports were based on nonrandomized uncontrolled case series.

## **HEPARIN**

Heparin treatment for CVT has been considered a standard therapy. Theories on the pathophysiology of CVT suggest a continuing process of disequilibrium between prothrombotic and thrombolytic mechanisms. Heparin treatment may act by shifting the equilibrium away from the prothrombotic action toward thrombolysis and inhibiting further thrombosis.

Two randomized trials and one meta-analysis of heparin treatment for CVT have been performed. The first trial, from Germany, was a randomized, blinded, placebo controlled study in 20 patients with dural sinus thrombosis. The trial was discontinued after 20 patients, because of significant differences in the recovery rate and mortality between the heparin and control group. The authors concluded that anticoagulation with dose-adjusted intravenous (IV) heparin (unfractionated heparin, bolus dose of 3000 IU and continuous infusion of 25,000-65,000 IU/day) was an effective treatment and an associated intracranial hematoma was not a contraindication for its use. This trial was criticized because its outcome assessment was not validated and there was a significant treatment delay after onset of symptoms. The trial failed to clarify the issue of duration of heparin treatment and the use of warfarin was questioned<sup>60-62</sup>. A randomized, placebo-controlled study from the Netherlands investigated the role of subcutaneous low-molecular-weight heparin (LMWH) in the management of CVT. In this study, 20% of patients in the heparin treatment group and 24% in the placebo group had a poor outcome after 3

weeks, and 13% in the treatment group and 21% in the placebo group had a poor outcome after 12 weeks. The definition of poor outcome was death or a Barthel index score of less than 15. This study did not demonstrate statistically significant clinical outcome improvement differences between the heparin treatment group and the control group; however, it revealed that the group treated with LMWH followed by oral anticoagulation showed a favorable outcome compared with the control group. The safety of anticoagulation was supported even in the setting of cerebral hemorrhage. A meta-analysis of the previously described two trials did not reveal a statistically significant improvement in outcome but demonstrated a 14.3% mortality reduction rate with heparin treatment and 15.5% risk reduction for death and dependency.

Heparin treatment remains a first-line treatment option in CVT because of the demonstrated safety of heparin and the favorable trend of clinical outcomes as shown in previous trials<sup>63</sup>.

## **INTERVENTION- ENDOVASCULAR TREATMENT**

Patients with a rapidly progressive thrombosis and diffuse brain swelling, with or without multiple hemorrhages, should be considered for endovascular thrombolytic therapy. It has been the authors' practice to start with at least 24 hours of heparin treatment. If clinical worsening of the patient's condition continues during that time period, endovascular thrombolytic therapy should be considered.

Since 1988, several reports have demonstrated the feasibility of direct infusion of thrombolytic agents into the thrombosed dural sinus by way of a percutaneous or retrograde transvenous approach<sup>64, 65</sup>. With improved catheter technology, it became possible to access and infuse thrombolytic agents into deep cerebral venous system. The potential benefit of local

administration of thrombolytic therapy is that it may avoid the systemic hemorrhagic effect caused by high-dose IV anticoagulation therapy. The technique of endovascular thrombolytic therapy has changed over the past decade, from a therapy of prolonged infusions of low dose urokinase (2 to 24 hours infusion, 0.5-20 million units) to a relatively rapid pulse-spray technique using recombinant tissue plasminogen activator (rtPA; 2-4 hours to administer 50-300 mg)<sup>66,67</sup>. The rtPA has many pharmacologic advantages over urokinase, including a short half-life, low antigenicity, and clot selectivity. The rtPA produces the lowest level of fibrinogen degradation products, which might contribute to the lower likelihood of hemorrhagic complications. These are two case series of local rtPA treatment with concomitant IV heparin treatments. Kim and Suh reported complete flow restoration in 18 hours and clinical improvement in all patients after rtPA treatment. They reported two nonneurologic rtPA-related complications (22.2%), including intrapelvic hematoma and puncture-site oozing but no intracranial hemorrhagic complication. **Frey et al.** showed flow restoration in 75% (complete in 50% and partial in 25%) of the patients within 29 hours of the rtPA treatment. They demonstrated that clinical recovery was closely related to the degree of flow restoration. In the group with complete flow restoration, 83% of patients had a complete clinical recovery. In the group with partial recanalization, 66% had a complete recovery. In the group that did not recanalize, only 33% demonstrated functional independence. The rtPA treatment resulted in neurologic deterioration in 16.7% of patients, who experienced enlargement of the parenchymal hematoma. These two series show that the local infusion of rtPA in CVT was technically feasible and flow restoration after rtPA treatment was important for future clinical outcome<sup>67</sup>. There is, however, a risk of clinical deterioration, especially in patients with intracranial hemorrhage.

At present, there does not exist a scientifically proven regimen of endovascular therapy that includes inclusion or exclusion criteria, dosage of thrombolytic agent, duration of treatment, concomitant usage of heparin, and a radiologic endpoint of the interventional procedure. Endovascular treatment can be performed only in highly sophisticated centers where interventional neuroradiologic expertise is available<sup>68</sup>. In the authors' institution, physicians perform endovascular treatment in patients who show clinical deterioration despite 24 hours of heparin therapy. The authors and other physicians in their institution use a rapid-pulsed direct-infusion technique of 30 to 50 mg of rtPA through a microcatheter over 15 to 20 minutes. The authors use concomitant IV heparin; their angiographic endpoint is antegrade flow within the dural sinus and not the total absence of thrombus within the dural sinus. In the authors' experience, the reestablishment of antegrade flow with continued anticoagulation is sufficient to facilitate clinical improvement.

Various dural sinus revascularization techniques other than local thrombolytic treatment have been reported, such as mechanical disruption using guide wires, rheolytic thrombectomy catheters, balloon thrombectomy with fibrinolysis, transluminal balloon angioplasty, with or without stenting, and surgical thrombectomy. The role of endovascular reopening of the dural sinuses using angioplasty and stent placement in the presence of severe intracranial venous hypertension is anecdotal and long-term results are not known<sup>69</sup>.

In conclusion, heparin is a first-line treatment option for CVT, and endovascular therapy should be considered if rapid clinical worsening occurs, despite anticoagulation. Endovascular treatment for CVT is feasible and effective in selected cases. Because the technology continues to improve, the potential role of endovascular treatment for CVT is promising.

Univariate analysis showed that heparin treatment was not related to outcome. Substantial number of patients with CVT may recover completely without any treatment. This study shows that the condition of the patient at the time of the diagnosis is far more important for the final outcome than whether the patient was treated with heparin. Endovascular thrombolytic therapy is reported as a safe and effective treatment for CVT in some uncontrolled case series, unless pretreatment cerebral haemorrhages are present, because it is invasive and potentially dangerous it should be considered only in patients with poor prognosis.

Overall prognosis of CVST is fairly good, at least for independent survival<sup>70</sup>. Coma and intracerebral haemorrhage are independent predictors for poor outcome, and involvement of the straight sinus is a possible additional unfavourable factor.



## **MATERIALS AND METHODS**

### **Source of data:**

This prospective study was performed on 34 patients diagnosed to have cerebral venous thrombosis over a period of 18 months from January 2014 to July 2015 in department of radiodiagnosis of R.L. Jalappa Hospital and Research Center attached to Sri Devaraj Urs Medical College, Kolar.

### **Method of collection of data:**

After an informed consent, patients in this study were scanned with 1.5 T MRI (Siemens Magnetom Avanto) in the department of radio diagnosis and examined with the following sequences:

- (1) T1, T2-weighted sequence.
- (2) Fluid-attenuated inversion recovery (FLAIR) sequence.
- (3) Diffusion-weighted imaging sequence with corresponding ADC mapping.
- (4) Susceptibility weighted imaging sequence.
- (5) 3-D time-of-flight imaging sequence.

ADC values were calculated automatically by the software and then displayed as a parametric map that reflected the degree of diffusion of water molecules through different tissues. Then ADC measurements were recorded for a given region by drawing regions of interest (ROIs) on

the ADC map. ADC values in the region of interest were compared with ADC values of the normal brain parenchyma.

Role of diffusion weighted imaging with ADC mapping in distinguishing type of edema, susceptibility weighted imaging to diagnose presence of any bleed and MR venogram to determine the extent of thrombus are also evaluated.

**Inclusion criteria:**

Any patient diagnosed to have cerebral venous thrombosis on MRI.

**Exclusion criteria:**

1. All patients with metallic implants and pacemakers.
2. Claustrophobic patients.

## **RESULTS**

34 patients who were diagnosed with cerebral venous thrombosis on MRI were included in the present study.

TABLE NO 3:

SEX WISE DISTRIBUTION IN PATIENTS WITH CEREBRAL VENOUS THROMBOSIS		
SEX	NO.OF CASES	PERCENTAGE (%)
MALES	15	44.1
FEMALES	19	55.9
TOTAL	34	100

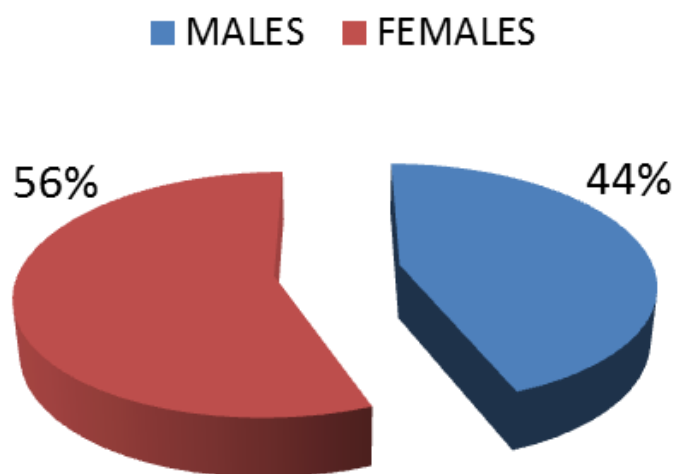
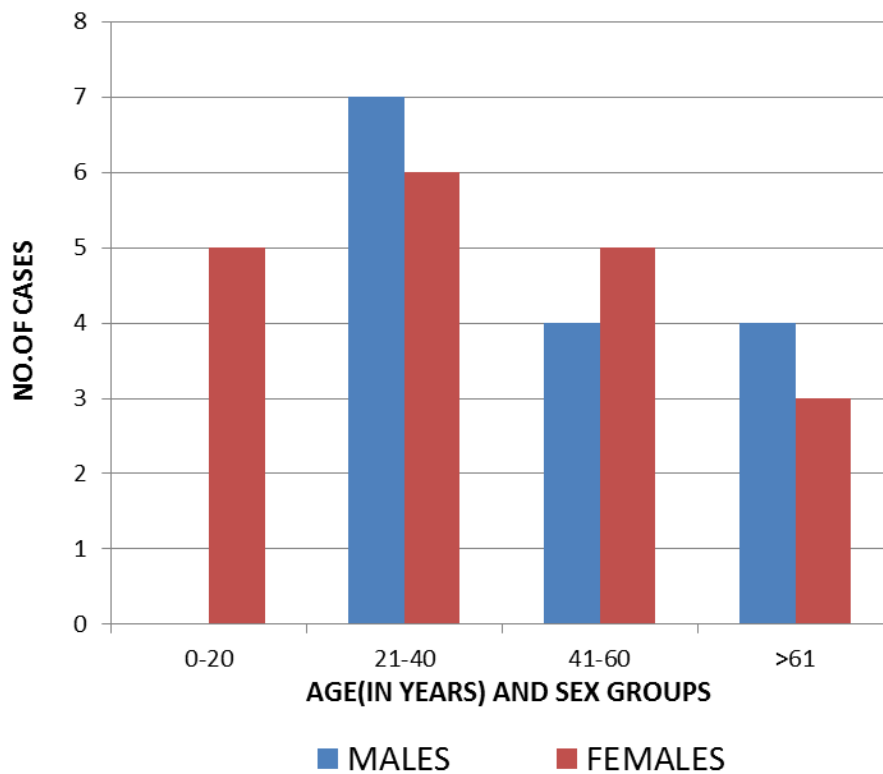


FIG 12: SEX WISE DISTRIBUTION

In the present study the female: male ratio is 1.3:1.

**TABLE NO. 4:**

AGE AND SEX WISE DISTRIBUTION IN PATIENTS WITH CEREBRAL VENOUS THROMBOSIS					
AGE (YEARS)	MALES		FEMALES		TOTAL NO.OF CASES
	CASES	%	CASES	%	
0-20	0	0	5	26.3	5
21-40	7	46.7	6	31.5	13
41-60	4	26.6	5	26.3	9
>61	4	26.6	3	15.7	7
<b>TOTAL</b>	<b>15</b>	<b>100</b>	<b>19</b>	<b>100</b>	<b>34</b>



**FIG 13: AGE AND SEX WISE DISTRIBUTION**

The peak incidence of cerebral venous thrombosis is seen in the age group of 21-40 years in both males and females (46.7% and 31.5% respectively).

TABLE NO.5:

DISTRIBUTION OF PATIENTS DEPENDING ON THE CAUSE IN PATIENTS WITH CEREBRAL VENOUS THROMBOSIS		
CAUSE	NO.OF PATIENTS	%
UNKNOWN	9	26.4
POSTPARTUM	9	26.4
DEHYDRATION	3	8.6
ORAL CONTRACEPTIVE PILLS	6	17.6
INTRACRANIAL SPACE OCCUPYING LESION	1	2.9
ALCOHOL	3	8.6
FEVER	2	5.8
SEPSIS	1	2.9
TOTAL	34	100

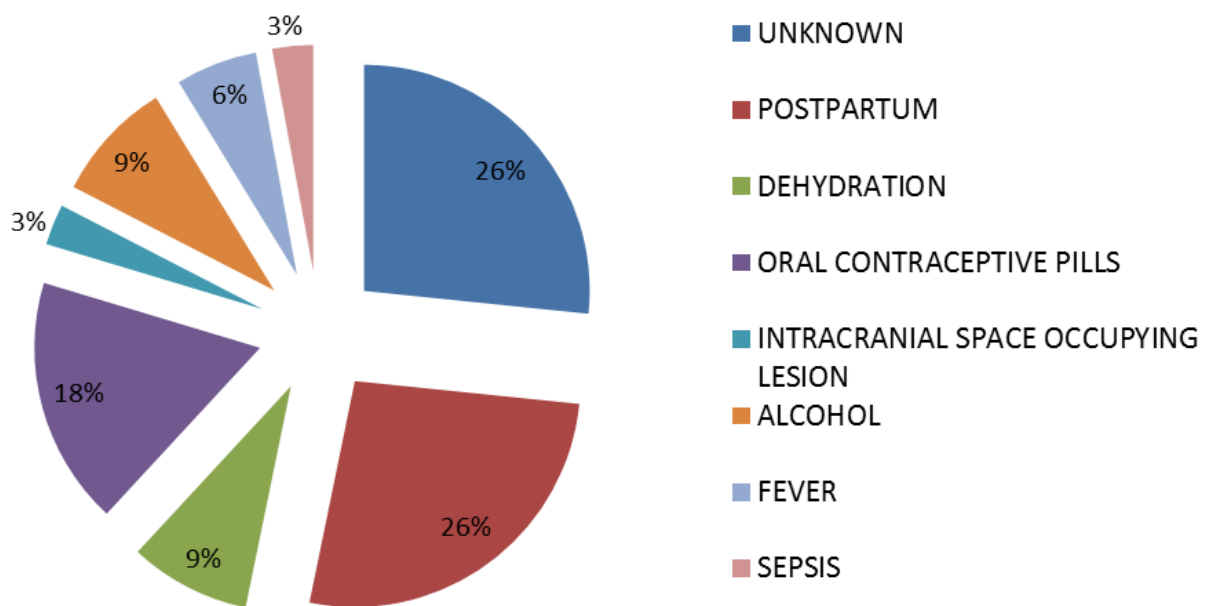


FIG 14: CAUSES OF CEREBRAL VENOUS THROMBOSIS

Out of 34 patients, Postpartum is the commonest cause for CVT which is seen in 9 patients (26.4%). The next common cause is oral contraceptive pills consumption constituting 6 patients (17.6%), followed by dehydration and alcohol, each constituting of 3 patients (8.6%). In 9 patients, cause was not known.

TABLE NO.6:

DISTRIBUTION OF PATIENTS BASED ON CLINICAL HISTORY IN PATIENTS WITH CEREBRAL VENOUS THROMBOSIS		
CLINICAL FEATURE	CASES	%
HEADACHE	10	29.4
HEMIPARESIS	7	20.5
GIDDINESS	3	8.8
SEIZURES	9	26.4
VOMITING	3	8.8
COMA	1	2.9
RAISED INTRACRANIAL TENSION	1	2.9
TOTAL	34	100

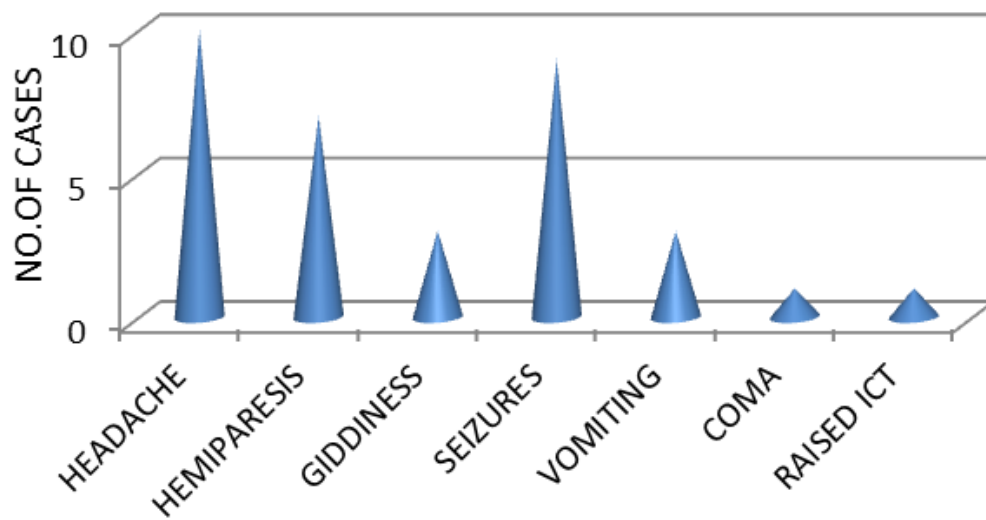


FIG 15: CLINICAL HISTORY IN PATIENTS OF CEREBRAL VENOUS THROMBOSIS

Headache is the commonest clinical feature seen in 10 patients (29.4%), the next common clinical feature being seizures in 9 patients (26.4%) followed by hemiparesis in 7 patients (20.5%).

TABLE NO.7:

DISTRIBUTION OF PATIENTS WITH CEREBRAL VENOUS THROMBOSIS DEPENDING ON THE EXTENT OF THROMBOSIS (NO.OF SINUSES INVOLVED IN EACH PATIENT)		
NO.OF SINUSES INVOLVED	CASES	%
ONE	11	32.3
TWO	13	38.2
THREE	8	23.6
FOUR	2	5.8
TOTAL	34	100

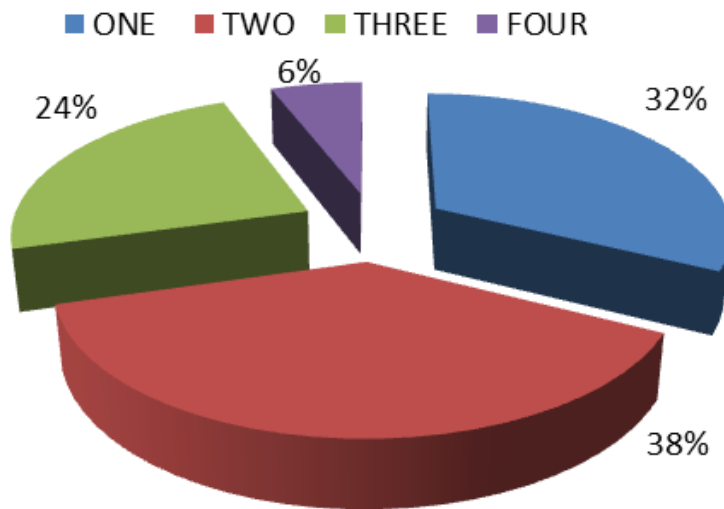


FIG 16: EXTENT OF THE THROMBOSIS

Present study revealed involvement of two sinuses in 12 patients (38.3%) and single sinus involvement is seen in 11 patients (32.3%), followed by three sinuses involvement in 8 patients (26.4%).

TABLE NO.8:

DISTRIBUTION OF PATIENTS WITH CEREBRAL VENOUS THROMBOSIS ACCORDING TO ASSOCIATED MANIFESTATIONS		
ASSOCIATED MANIFESTATION	NO.OF CASES	%
HAEMORRHAGIC INFARCT	16	47
NON-HAEMORRHAGIC INFARCT	13	38.2
INTRACEREBRAL HAEMATOMA	5	14.8
TOTAL	34	100

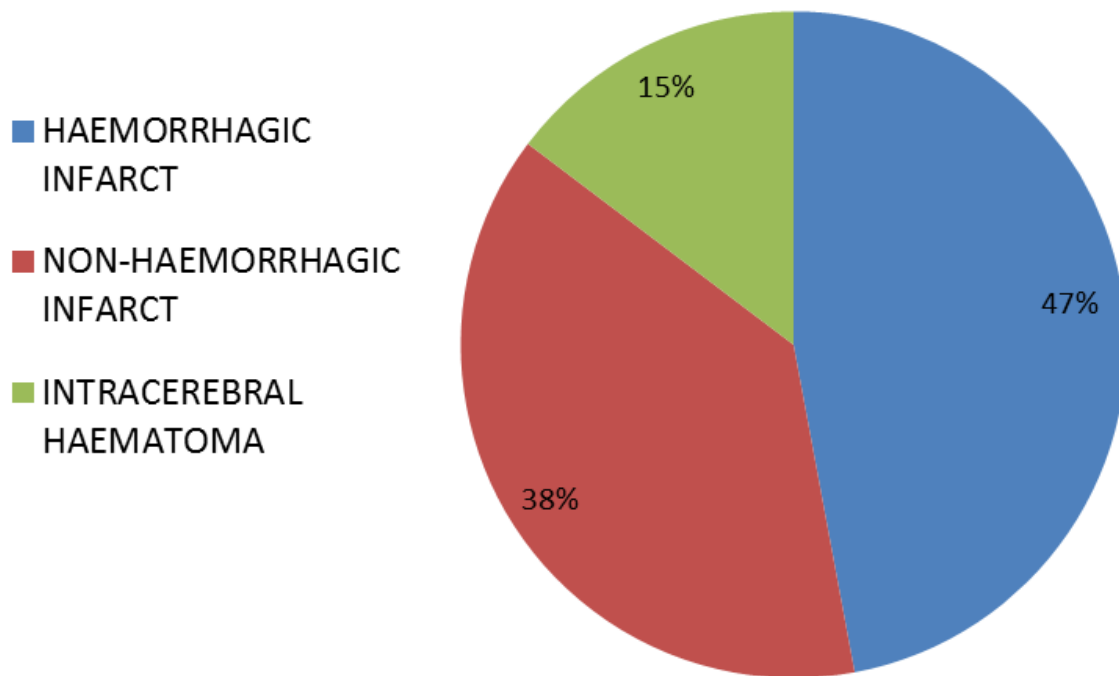


FIG 17: ASSOCIATED MANIFESTATIONS

Hemorrhagic infarct is the most common associated manifestation seen in 16 patients (47%) followed by non-hemorrhagic infarct in 13 patients (38.2%) and intracerebral hematoma in 5 patients (14.8%)



**TABLE NO.9:**

DISTRIBUTION OF SINUSES INVOLVED IN PATIENTS OF CEREBRAL VENOUS THROMBOSIS		
SINUS	NO.OF CASES	%
SUPERIOR SAGITTAL SINUS	15	21.7
INFERIOR SAGITTAL SINUS	3	4.3
STRAIGHT SINUS	10	14.4
TRANSVERSE SINUS	19	27.8
CAVERNOUS SINUS	2	2.8
VEIN OF GALEN	4	5.8
CORTICAL VEINS	4	5.8
SIGMOID SINUS	6	8.7
INTERNAL JUGULAR VEIN	6	8.7

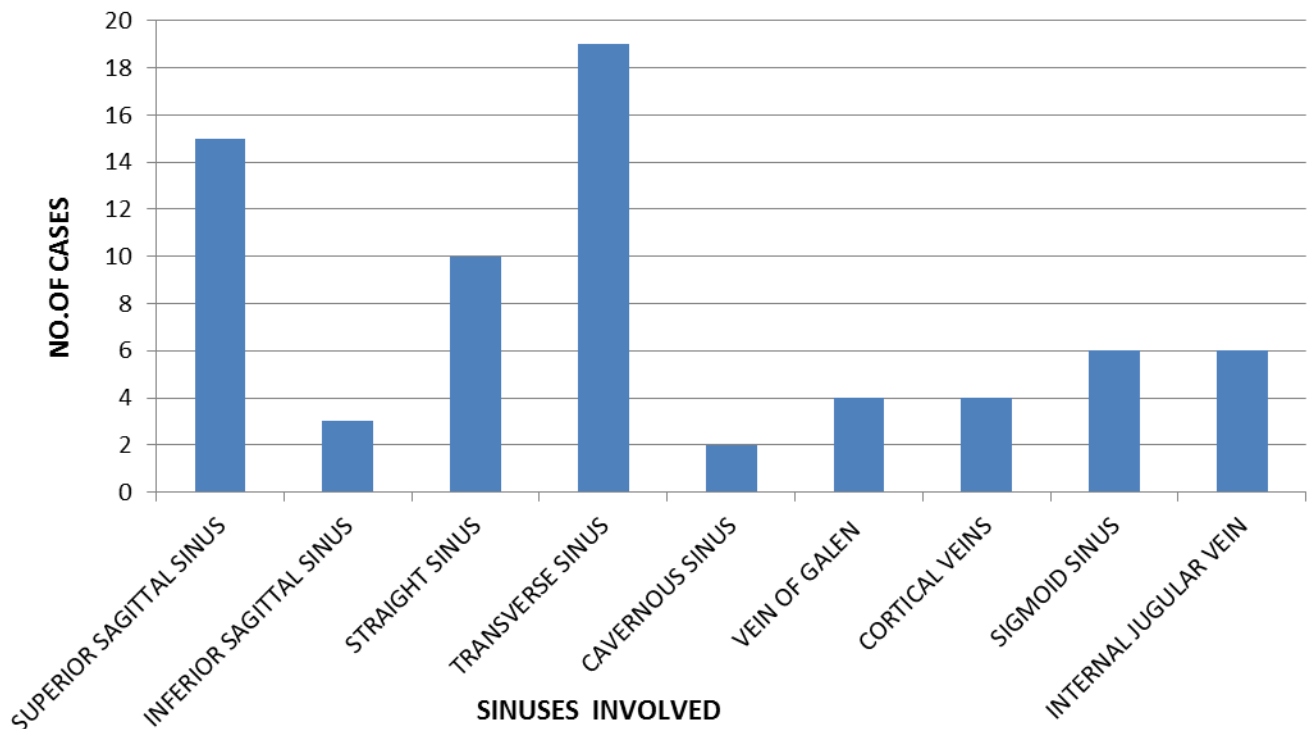
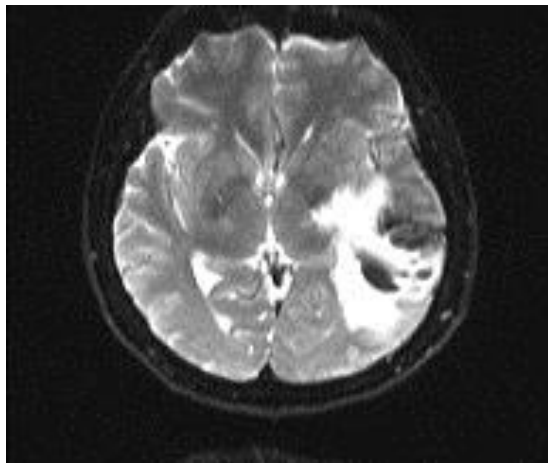
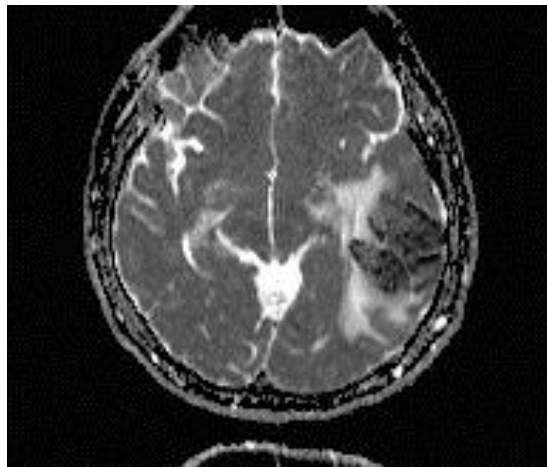


**FIG 18: SINUSES INVOLVED**

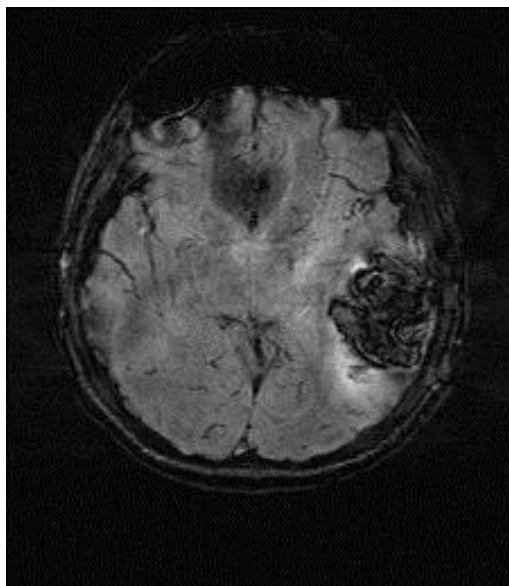
In the present study, transverse sinus is most commonly involved in cerebral venous thrombosis which is seen in 19 patients (27.8%). The next commonest sinus involved is superior sagittal sinus in 15 patients (21.7%) followed by straight sinus in 10 patients (14.4%).



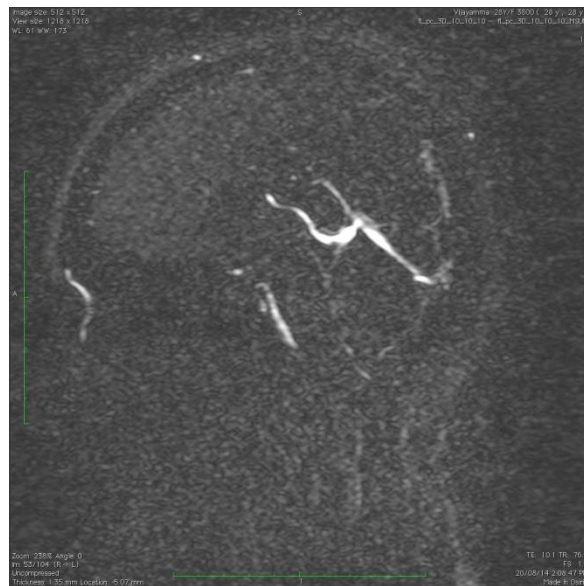
(A)



(B)



(C)

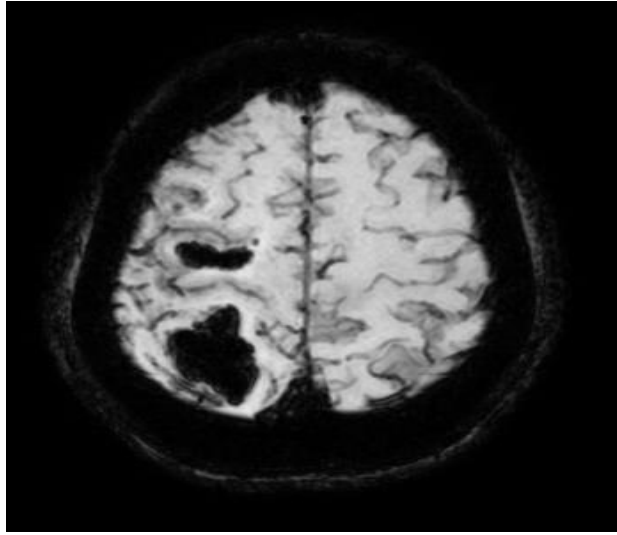


(D)

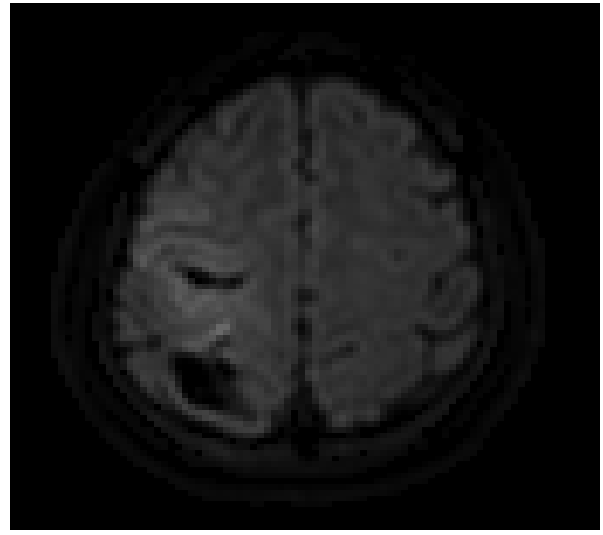
**A 23 year old female patient in postpartum status presented with seizures and altered sensorium.**

**FIG 19: A & B: DWI and ADC images showing infarct in left temporo-parietal regions.**

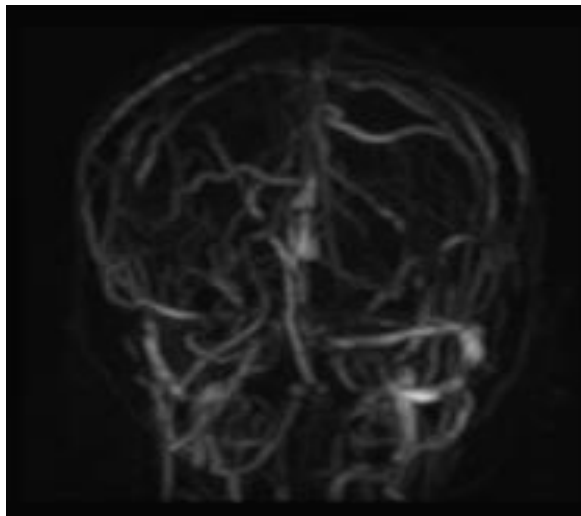
**FIG C: SWI showing blooming within the area of infarct confirming it to be a hemorrhagic infarct. FIG D: Sagittal 2D TOF image showed absence of flow signals in superior sagittal sinus, transverse sinus and sigmoid sinus**



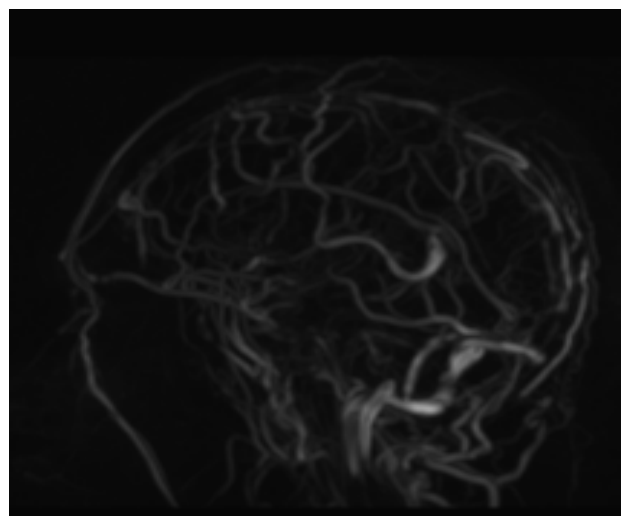
(A)



(B)



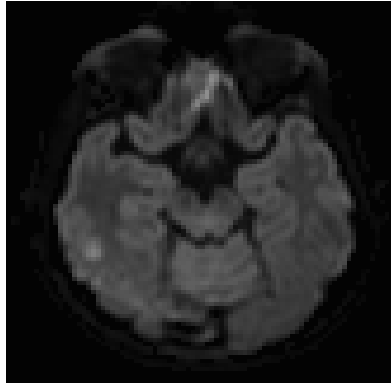
(C)



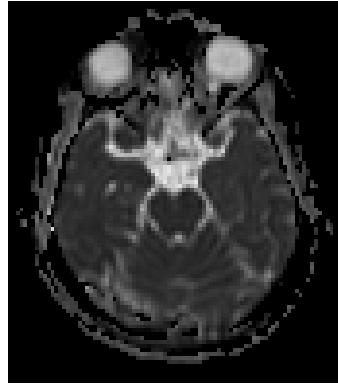
(D)

**A 56 years old male presented with left sided hemiparesis.**

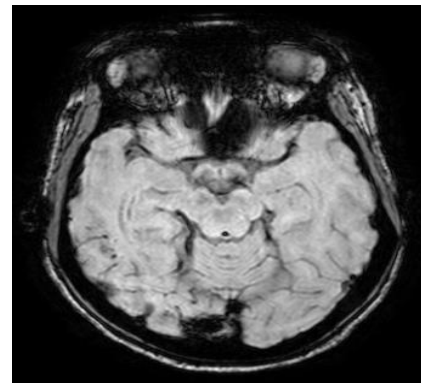
**FIG 20: A&B: - SWI and DWI showing haemorrhagic infarcts in the right frontal and parietal lobes. C&D: MRV shows loss of normal flow voids with filling defects in post contrast images in superior sagittal, right transverse, sigmoid sinuses, internal jugular vein and distal straight sinuses.**



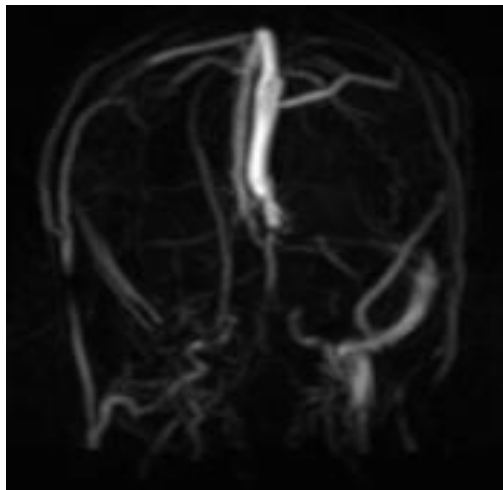
(A)



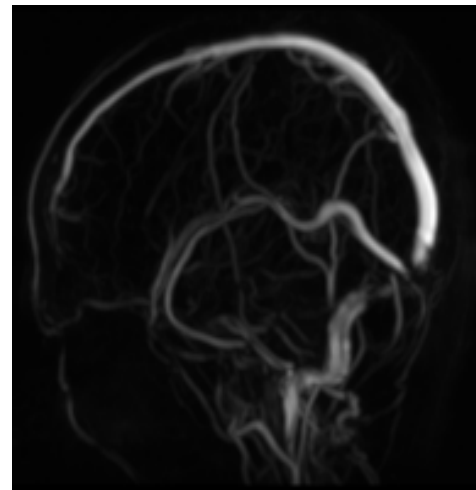
(B)



(C)



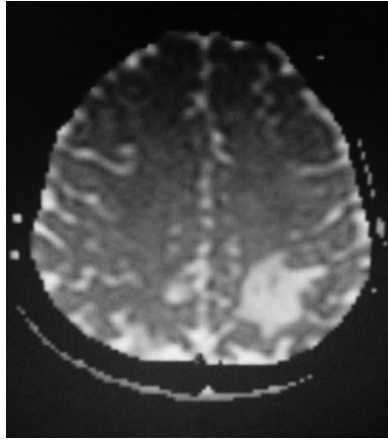
(D)



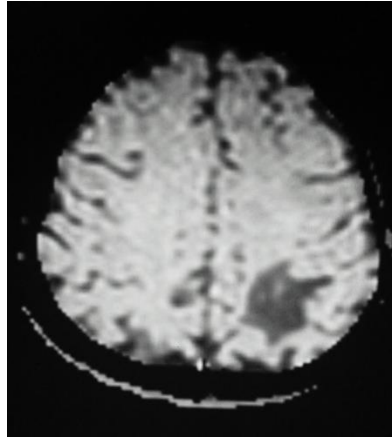
(E)

**19 years old female presented with postpartum seizures ,**

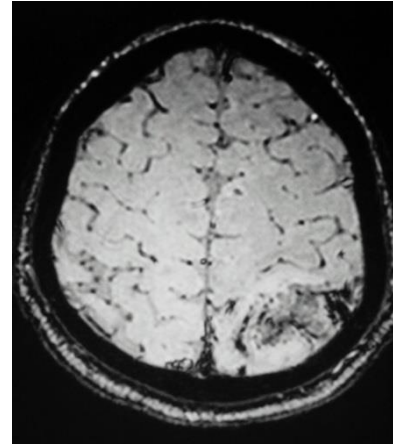
**Fig 21: A& B: DWI and ADC images showing infarct in right inferior temporal lobe. (C) SWI shows blooming within the area of infarct confirming it as hemorrhagic infarct. (D) & (E) MRV Coronal and sagittal 2D TOF MIP images showed absence of flow signals in distal superior sagittal, right transverse, sigmoid sinuses, internal jugular vein, left proximal transverse and sigmoid sinuses.**



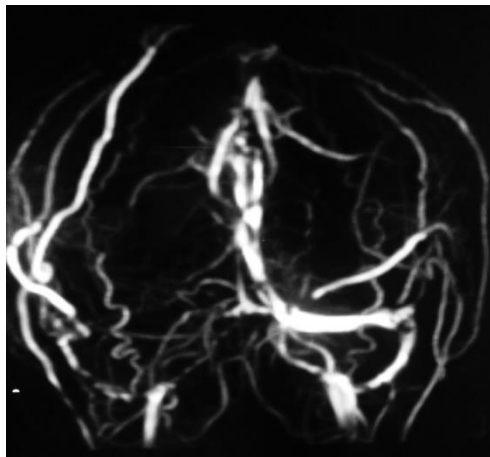
(A)



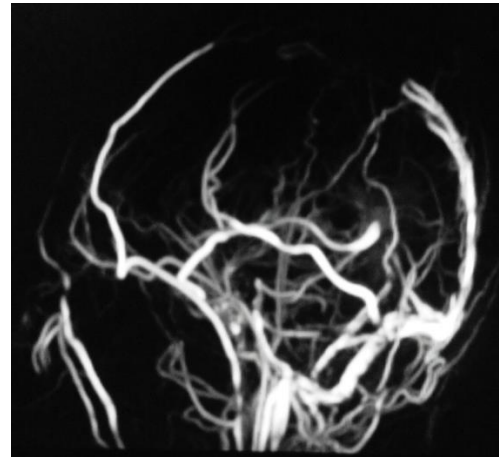
(B)



(C)



(D)



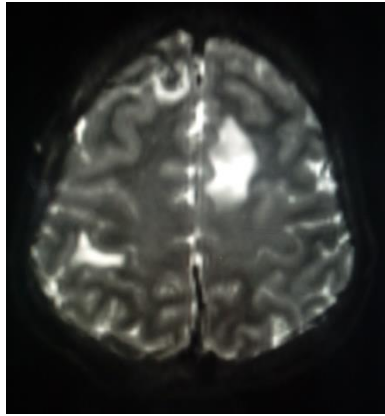
(E)

**A 35 year old male patient presented with right sided hemiparesis.**

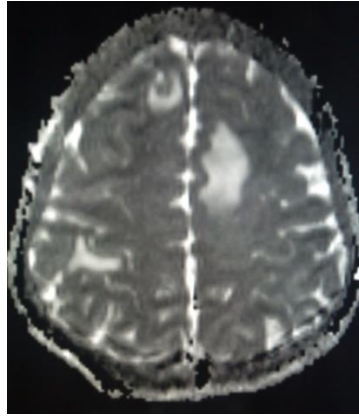
**FIG 22: A&B DWI and ADC images showing infarct in left parietal lobe.**

**FIG C: SWI showing blooming within the area of infarct and confirms it to be a hemorrhagic infarct.**

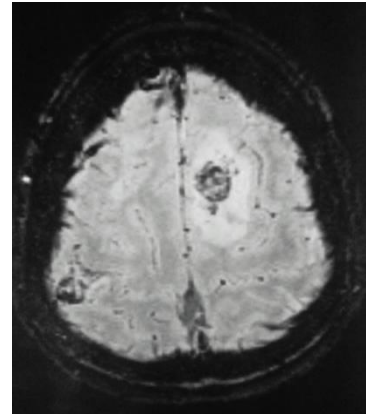
**FIG D&E: MRV shows multiple filling defects in superior sagittal sinus, right transverse, sigmoid sinuses and proximal IJV.**



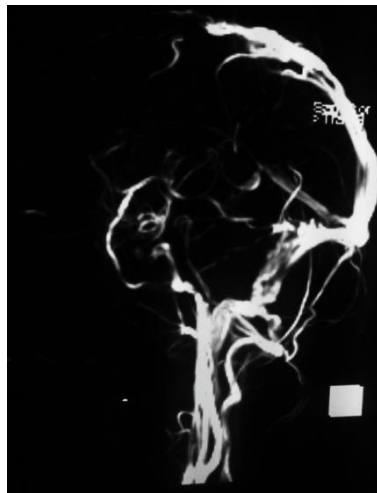
(A)



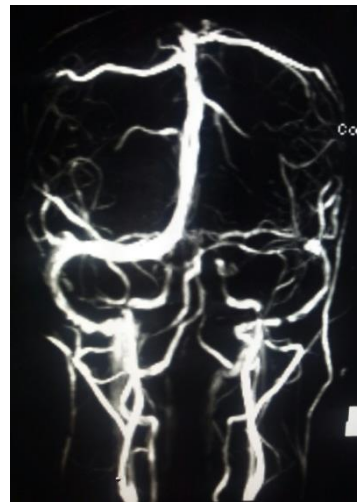
(B)



(C)



(D)



(E)

**A 70 year old female presented with sudden loss of consciousness.**

**FIG 23: A, B&C: DWI images shows hyperintensities in bilateral frontal lobes, ADC confirms no restriction. SWI shows blooming within the concerned areas and confirms it to be hemorrhages. FIG D& E: MRV shows non visualization of anterior part of superior sagittal sinus and hypoplastic left transverse sinus.**

## **DISCUSSION**

Cerebral venous thrombosis refers to occlusion of venous channels in the cranial cavity, including dural venous, cortical and deep cerebral veins. This disorder is potentially lethal but treatable, often it was overlooked in both clinical and radiologic routine practice. MR Venogram, SWI and DWI with ADC mapping are useful methods to establish the diagnosis. These imaging modalities may reveal either direct sign of visualization of intraluminal clot or indirect signs such as parenchymatous change and intracranial hemorrhage.

CVT is believed to be more common in women than men. . Female predominance is seen in our study where female to male ratio is 1.3: 1. In a series of 110 cases, **Ameri and Bousser** found a female-to-male ratio of 1.29:1<sup>71</sup>. **Ferro et al.** made the same observations in a prospective study from 1995 to 1998. This slight preponderance in females is probably due to specific causes such as oral contraceptives, pregnancy and puerperium. This preponderance of females did not exist before the era of the oral contraceptive pills<sup>72</sup>.

CVT is more frequent in age group of 20-35 years. In our study, 42.8 % patients had CVT in the age group of 21 to 40 years. According to an Indian study, it is a major cause of stroke in young population with a mean age of 32.27 years and therefore should be considered in all cases of young stroke<sup>73</sup>. In 1992, **Ameri and Bousser** reported a uniform age distribution in men with CVT, while 61% of women with CVT were aged between 20-35 years<sup>71</sup>.

The commonest causes of CVT based on clinical history in our study are post-partum (26%), oral contraceptive pills (17.6 %) and alcohol (9%) whereas cause could not be identified in 27 %

cases of CVT. According to extensive investigations conducted by **Ameri and Bousser**, no cause was identified in 20-25 % cases. Pregnancy and puerperium have been recognized as periods of increased susceptibility<sup>71</sup>.

The symptomatology and clinical findings are variable depending on site of thrombosis. In the present study headache was seen in 29.4 % of patients 26.4 % of patients had seizures of which generalized tonic clonic type was commonest and 21% patients had hemiplegia. Headache appeared to be common in cerebral venous thrombosis, varying from 29% to 57.8%<sup>73</sup>

**Carrol et al** found seizures in 29.83% of patients<sup>74</sup>, **Srinivasan and Natarajan** found seizures in 66% patients<sup>75</sup>. **Nagaraja et al** found seizures in 26.6%. Hemiplegia is a common presenting complaint noticed in various series<sup>75</sup>.

In present study transverse sinus was the most common sinus involved in 27.8 % cases followed by superior sagittal sinus in 22 % cases, straight sinus in 14.4 % and sigmoid sinus in 9 % cases. Overall, 66.7 % cases showed involvement of more than one sinus. In a study done by **Sanjay M Khaladkar et al.** in 2014 the most common sinus involved was superior sagittal sinus with almost equal involvement of transverse and sigmoid sinuses . The deep venous system was affected in 17.5% patients, and superficial venous system affected in 2.5% of cases. Most of the patients had involvement of more than one sinus<sup>55</sup>. **Greiner et al.** concluded that in veno-occlusive stroke, the superior sagittal sinus followed by transverse, sigmoid, and straight were generally involved<sup>56</sup>.

In our study, all cases of cerebral venous infarct showed restriction on DWI. The areas of hyperintensities on DWI also showed T2 signal changes. This is explained by image timing, because we did not image any subject hyperacutely when diffusion restriction might have been



present in the absence of T2 hyperintensity .This might also be due to interval between the time from onset of disease to time of MRI. This time interval can be attributed to diverse clinical manifestations of CVT.

We demonstrated the ADC changes in all 34 patients with cerebral venous thrombosis. The results indicate that vasogenic edema develops more frequently and earlier in cerebral venous thrombosis. Though both vasogenic and cytotoxic edema are associated with the pathological condition of the disease, vasogenic edema is prominent in the early phase of CVT. **Kon Chu et al** showed coexistence of increased and decreased ADCs with that of disease progression. One case report on straight sinus and deep cerebral venous thrombosis described a local augmentation of ADC, which was in correlation to our results<sup>76</sup>. Increase in ADC suggests predominance of vasogenic edema in the early phase of the CVT. It was reported that the reduction in ADC persisted upto 6 days on average after stroke due to arterial ischemia and a significant reduction of ADC was detected for at least 4 days<sup>77</sup>. ADC changes in the early phase of dural sinus thrombosis differ from those of arterial ischemia, in which cytotoxic edema is predominant in the hyperacute or acute phase.

Parenchymal hemorrhages were seen in 16 patients in our study. **James L et al** concluded in a study in 2006 that the mechanism of hemorrhage is multifactorial. Hemorrhage may be precipitated by continued arterial perfusion in areas of cell death similar to reperfusion in arterial ischemia. Elevation of venous pressure beyond the limit of venous wall is also believed to be a cause<sup>78,79</sup>.

In current study all patients with hemorrhagic venous infarcts and intracerebral hematoma were diagnosed by blooming on SWI. The reason being that SWI is exquisitely sensitive to paramagnetic substances, such as deoxygenated blood, blood products, iron, and calcium. A similar study conducted in 2010 also concluded that thrombosed sinuses have deoxyhemoglobin, which can be readily detected on SWI by the presence of hypointensity and blooming<sup>80</sup>. Venous infarcts are frequently hemorrhagic and SWI assists in detecting even small hemorrhages in venous infarcts.

Diffusion weighted imaging and ADC measurement of intracranial hematoma were recently reported by **Atlas et al** , however in our study ADC values of hematoma have not been evaluated. The reason being, the determining factors of ADC values in hematoma may be due to paramagnetic effect of the methemoglobin rather than true restriction of water movement<sup>79</sup>.

Although many studies shows significant occurrence of hemorrhagic infarct in presence of CVT, no study clearly explains the incidence of hemorrhagic venous infarcts in CVT<sup>76</sup>. The present study shows hemorrhagic venous infarcts in 47 % cases.

Multiple locations of thrombosis were identified, in majority of the cases (n=19) transverse sinus was affected; the associated parenchymal involvement was ipsilateral parieto-temporal lobes. Superior Sagittal sinus involvement was seen in 15 cases and the associated parenchymal involvements were unilateral or bilateral fronto-parietal lobes. The parenchymal abnormalities that occurred with deep venous occlusion were thalami and deep periventricular regions. Cortical

venous involvements were seen in 4 cases. However the correlation of parenchymal changes with extent of venous sinus involvement was variable.

Thrombus on MRV was seen either as loss of high flow signals from the sinus, in cases of complete occlusion of the sinus or frayed and patchy flow signal in partial thrombosis. In our study shows 23 out of 34 patients showed thrombus involving more than one sinus. This is in correlation with recent study done by **Sanjay M Khaladkar et al** in which majority of cases showed involvement of more than one sinus<sup>55</sup>.

## **CONCLUSION**

Cerebral venous sinus thrombosis is a challenging condition because of its variability of clinical symptoms and signs. It is very often unrecognized at initial presentation. All age groups can be affected. The prognosis of cerebral venous sinus thrombosis is generally favorable, that makes early and accurate diagnosis of CVT very crucial.

Our study demonstrated the role of MRI with MR venogram, diffusion weighted imaging with ADC mapping and susceptibility weighted imaging in early and accurate diagnosis of cerebral venous thrombosis.

MRI and MRV were efficacious in detecting cerebral venous sinus thrombosis and brain parenchymal abnormalities due to CVT. These help in early detection and management of CVT to avoid neurological deficit. Thrombus on MRV was seen either as loss of high flow signals in cases of complete occlusion or frayed and patchy flow signal in the presence of partial thrombosis.

DWI with ADC maps can be used to discriminate between types of edema for tissue viability and to provide diagnostic clues in CVT. The results of our study indicate that though both vasogenic and cytotoxic edema are associated in the early phase of CVT, vasogenic edema develops more frequently. Our study showed variable ADC values in all cases. Increase in ADC suggests predominance of vasogenic edema and decrease in ADC suggests cytotoxic edema.

The study also demonstrates that susceptibility-weighted imaging is an important technique that allows accurate detection of early hemorrhagic transformations within acute infarctions. It also detects chronic microbleeds and intracerebral hematomas, thus helping to decide the treatment protocol.

## **SUMMARY**

Cerebral venous thrombosis (CVT) is a rare form of stroke. It is commonly seen in young and middle aged group, especially in women. It causes acute neurological deterioration with increased morbidity and mortality if not diagnosed in early stage. Neurological deficit occurs due to focal or diffuse cerebral edema and non-hemorrhagic / hemorrhagic venous infarct.

The aims of the study were to study the role of MRI with MR venogram, diffusion weighted imaging with ADC mapping and susceptibility imaging in diagnosis of cerebral venous thrombosis.

The study was carried out in 34 patients who were diagnosed to have CVT from January 2014 to July 2015 in the department of Radiodiagnosis of R L Jalappa Hospital and Research Centre, Tamaka, Kolar.

The study show that MRI with MR venogram, diffusion weighted imaging with ADC mapping and susceptibility weighted imaging are used to evaluate extent of thrombus, differentiate between the type of edema, detect presence of hemorrhage and deliver time-saving information for diagnosis of CVT.

There was female preponderance in the study. The most common affected age group was 21-40 years for both genders.

Hemorrhagic venous infarct was the most common associated manifestation in our study comprising 47 % of cases.

The cause for CVT remained unknown in 9 patients. The most common cause for CVT in our study was post-partum status, use of oral contraceptives in females and alcoholism in males.

The most common clinical feature in the patients was headache followed by seizures and hemiparesis.

Most commonly affected sinus was transverse and superior sagittal sinuses (27.8% and 21.7 % respectively). 23 patients (63.7%) in our study showed involvement of more than one sinus.

The results of the study strongly support the role of MRI with MR venogram, diffusion weighted imaging and susceptibility weighted imaging in early and accurate diagnosis of CVT and its associated findings.

## **BIBLIOGRAPHY**

1. Rother J Waggie Kvan Bruggen Nde Crespigny AJMoseley ME Experimental cerebral venous thrombosis: evaluation using magnetic resonance imaging. J Cereb Blood Flow Metab.1996;16:1353-1361.
2. R.V. Damadian "Tumor detection by Nuclear Magnetic Resonance." Science 1971 ; 171: 1151.
3. Thomas S Curry, James E Dowdey, Robert E Murry Jr. Christensen's Physics of Diagnostic Radiology, 4<sup>th</sup> Edn: Nuclear Magnetic Resonance, August 1990;32:432
4. Kumar A, D.Welti, R.R Ernst "NMR Fourier zeugmatography". J. Magn. Reson 1975; 62:34.
5. P Mansfield "Multi-planar image formation using NMR spin-echoes". J Phys. C:Solid State Physics 1977;10: 55-58.
6. B.Chapman, R.Turner, R.J. Ordidge, M. Doyle, M. Cawley, R. Coxon, P.Glover, P.Mansfield "Real-Time Movie Imaging from single cardiac cycle by NMR". Magn. Reson. Med 1987; 5:246-254.
7. C.L. Dumolin, S.P. Souza, H.R. Hart "Rapid Scan Magnetic Resonance Angiography". Magn. Reson. Med. 1987; 5:238-245.
8. K.K Kwong, J.W. Belliveau, D.A. Chesler, I.E. Goldberg, R.M. Weisskoff, B.P. Ponchelet, D.N. et al. Dynamic magnetic resonance imaging of human brain activity during primary sensory stimulation. Proc Natl. Acad. Sci. 1992;89:5675.
9. M.S. Albert, G.D. Cates, B. Driehuys, W.Happer, B. Saam, C.S. Springer Jr., A. Wishnia "Biological magnetic resonance imaging using laser-polarized  $^{129}\text{Xe}$ ". Nature 1994;370:199-201.



10. Martyn NJ Paley, Iain D Wilkinson, Edwin van Beek and Pauk D Griffiths. Grainger and Allison's Diagnostic radiology. A textbook of Medical Imaging 4<sup>th</sup> Edn. Magnetic Resonance Imaging: Basic principles 2001; 5:101-102.
11. Ozvath RR, Casey SO, Lustrin ES, et al. Cerebral Venography: Comparison of CT and MR projection venography. Am J Roentgenol 1997; 169:1699-707.
12. James N. Scott, Richard I. Farb, Imaging and anatomy of the normal intracranial venous system. Neuroimaging Clin N Am 2003; 13:1-12.
13. Wehrli FW: Parameters determining the appearance of NMR images. In Newton TH, Potts DG(eds): Advanced Imaging Techniques. San Anselmo, CA, Clavadel Press, 1983:159-186.
14. Dixon RL, Ekstrand KE: The Physics of proton NMR. Med Physics 1982;9:807-815.
15. Gore JC: The meaning and significance of relaxation in NMR imaging. In Witkofshi RL, Karstaedt N, Partain CL (eds): NMR Imaging: Proceedings of an International Symposium. Winston-Salem, NC, Bowman Gray School of Medicine, Wake Forest University 1982:147-157.
16. Lasjaunias P, Berenstein A, Brugge KG, et al. Intracranial venous system. Surgical neuroangiography. Ed 2. Berlin: Springer-Verlag; 2001. 631– 695.
17. Ture U, Yasargil MG, Al-Mefty O. The transcallosal transforminal approach to the third ventricle with regard to the venous variations in this region. J Neurosurg 1997;87:706–15.
18. Bisaria KK. Anatomic variations of venous sinuses in the region of the torcular Herophili. J Neurosurg 1985; 62: 90-95.
19. Cure JK, Van Tassel P, Smith MT. Normal and variant anatomy of the dural venous sinuses. Semin Ultrasound CT MRI 1994;15(6):499-519.

20. Mamourian AC, Towfighi J. MR of giant arachnoid granulations: a normal variant presenting as a mass within the dural venous sinus. *Am J Neuroradiol* 1995; 16: 901-4.
21. Roche J, Warner D. Arachnoid granulations in the transverse and sigmoid sinuses: CT, MR and MR angiographic appearance of a normal anatomic variation. *Am J Neuroradiol* 1996; 17:677-83.
22. Leach JL, Jones BV, Tomsick TA, et al. Normal appearance of arachnoid granulations on contrast enhanced CT and MR of the brain: Differentiation from dural sinus disease. *Am J Neuroradiol* 1996;17:1523-32.
23. Lee SK, Kim BS, Terbrugge K. Clinical presentation, imaging and treatment of cerebral venous thrombosis (CVT). *Intervent Neuroradiol* 2002;8: 5– 14.
24. Poon CS, Chang JK, Swarnkar A, et al. Radiologic diagnosis of cerebral venous thrombosis: pictorial review. *Am J Radiol.* 2007;189:S64–S75.
25. Prakash C, Bansal BC. Cerebral venous thrombosis. *J India Aca Clin Med.* 2000;5:55–61.
26. Rodallec MH, Krainik A, Feydy A, et al. Cerebral venous thrombosis and multidetector CT angiography: tips and tricks. *RadioGraphics.* 2006;26:S5–S18.
27. Leach JL, Strub WM, Gaskill-Shipley MF. Cerebral venous thrombus signal intensity and susceptibility effects on gradient recalled-echo MR imaging. *Am J Neuroradiol.* 2007;28:940–5
28. Linn J, Pfefferkorn T, Ivanicova K, et al. Noncontrast CT in deep cerebral venous thrombosis and sinus thrombosis: comparison of its diagnostic value for both entities. *Am J Neuroradiol.* 2009:A1451–A1451.

29. Wasay M, Kojan S, Dai AI, Bobustuc G, Sheikh Z. Headache in Cerebral Venous Thrombosis: incidence, pattern and location in 200 consecutive patients. *J Headache Pain*. 2010 Apr. 11(2):137-9.
30. Denise M. Lemke;Lofti Hacein-Bey *J NeurosciNurs*. 2005;37(5):258-264.
31. Van Gijn J. Cerebral venous thrombosis: pathogenesis, presentation and prognosis. *J R Soc Med* 2000; 93:230–233.
32. Connor SEJ, Jarosz JM. Magnetic resonance imaging of cerebral venous sinus thrombosis. *Clin Radiol* 2002;57:449–461.
33. Colin S. Poon<sup>1,2</sup>, Ja-Kwei Chang<sup>1</sup> , Amar Swarnkar<sup>1</sup> , Michele H. Johnson , John Wasenko<sup>1</sup> Radiologic Diagnosis of Cerebral Venous Thrombosis: Pictorial Review. *AJR* 2007;189:S64–75.
34. Katarzyna Sklinda. Neuroimaging of Cerebral Venous Thrombosis (CVT) – Old Dilemma and the New Diagnostic Methods. *Polish Journal of Radiology* 2015; 80: 368-373.
35. Masuhr F, Mehraein S, Einhaupl K. Cerebral venous and sinus thrombosis. *J Neurol* 2004;251: 11–23.
36. Karthikeyan D, Vijay S, Kumar T, et al. Cerebral venous thrombosis-spectrum of CT findings. *Neuroradiology*. 2004;14:129–37.
37. Aliasgar V, Moiyadi M Ch, Indira Devi B. Posttraumatic non-sinus cerebral venous thrombosis. *Indian J of Neurotrauma*. 2006;3:143–146.
38. Meckel S, Reisinger C, Bremerich J, et al. Cerebral venous thrombosis: diagnostic accuracy of combined, dynamic and static, contrast-enhanced 4D MR venography. *Am J Neuroradiol*. 2010;31:527–35.

39. Crombe D, Haven Fr, Gille M. Isolated deep cerebral venous thrombosis diagnosed on CT and MR imaging. a case study and review literature. JBR–BTR. 2003;86:257–61.
40. Manzione J, Newman GC, Shapiro A, Santo-Ocampo R. Diffusion- and perfusion-weighted MR imaging of dural sinus thrombosis. AJNR Am J Neuroradiol 2000;21:68–73.
41. Keller E, Flacke S, Urbach H, et.al: Diffusion- and perfusion weighted magnetic resonance imaging in deep cerebral venous thrombosis. Stroke 1999; 30:1144-46.
42. Ahmed Idbaih, Monique Boukobza, Isabelle Crassard. MRI of Clot in Cerebral Venous Thrombosis:High Diagnostic Value of Susceptibility-Weighted Images. Stroke.2006; 37: 991-995.
43. Hingwala D, Kesavadas C, Thomas B, Kapilamoorthy TR. Clinical utility of susceptibility-weighted imaging in vascular diseases of the brain. Neurol India. 2010;58: 602–7.
44. Tsui YK, Tsai FY, Hasso AN, Greensite F, Nguyen BV. Susceptibility-weighted imaging for differential diagnosis of cerebral vascular pathology: A pictorial review. J Neurol Sci. 2009;287:7–16.
45. Santhosh K, Kesavadas C, Thomas B, Gupta AK, Thamburaj K, Kapilamoorthy TR. Susceptibility weighted imaging: A new tool in magnetic resonance imaging of stroke. Clin Radiol. 2009;64:74–83.
46. Meckel S, Reisinger C, Bremerich J, et al. Cerebral venous thrombosis: diagnostic accuracy of combined, dynamic and static, contrast-enhanced MR venography. Am J Neuroradiol. 2010;31:527–35.

47. Stam J. T Leach JL, Fortuna RB, Jones BV, Gaskill-Shipley MF. Imaging of cerebral venous thrombosis: Current techniques, spectrum of findings, and diagnostic pitfalls. *Radiographics* 2006;26:S19-41. Thrombosis of the cerebral veins and sinuses. *N Engl J Med* 2005;352:1791-8.
48. Teasdale E. Cerebral venous thrombosis: making the most of imaging. *J R Soc Med.* 2000;93:234–37.
49. Lovblad, Karl-Olof A, Basseti, Claudio B, Schneider, Jacques A. Diffusion-weighted MR in Cerebral Venous Thrombosis: *Cerebrovascular Diseases* 2001;11(3) :169-176.
50. Bousser MG. Cerebral Venous Thrombosis: Diagnosis and management. *J Neurol* 2000;247:252-258.
51. Manzione J, Newman GC, Shapiro A, Santo-Ocampo R: Diffusion and Perfusion weighted MR imaging of dural sinus thrombosis. *Am J Neuroradiol* 2000; 21:68-73.
52. Ebisu T, Naruse S, Horikawa Y, et al. Discrimination between different types of white matter edema with diffusion weighted MR imaging. *J Magn Reson Imaging* 1993;3(6):863-868.
53. Kon Chu, MD; Dong-Wha Kang, MD, PhD; Byung-Woo Yoon, MD, PhD; Jae-Kyu Roh, MD, PhD: Diffusion weighted magnetic resonance in cerebral venous thrombosis: *Arch Neurol* 2001;58: 1569-1576.
54. Marie-Germaine Bousser, José M Ferro. Cerebral venous thrombosis: an update. *Lancet Neurol.* 2007;6(2):162–70.
55. Khaladkar SM, Thakkar DK, Thakkar DK, Shrotri H, Kulkarni VM. Cerebral venous sinus thrombosis on MRI: A case series analysis. *Med J DY Patil Univ* 2014; 7:296-303
56. Greiner FG, Takhtani D. Neuroradiology case of the day. Superior sagittal sinus thrombosis and infarcts. *Radiographics* 1999;19:1098-1101.

57. Karthikeyan D, Vijay S, Kumar T, Kanth L. Cerebral venous thrombosis-spectrum of CT findings. *Ind J Radiol* 2004;14:129-37.
58. Kolacki, C. and Rocco, V. (2012) The combined vaginal contraceptive ring, nuvaring, and cerebral venous sinus thrombosis: A case report and review of the literature. *The Journal of Emergency Medicine*, 42, 413-416.
59. Maurice Preter, ; Christophe Tzourio, MD; Alain Ameri, *Stroke*.1996; 27: 243-246.
60. Benamer HT, Bone I. Cerebral venous thrombosis: anticoagulants or thrombolytic therapy. *J Neurol Neurosurg Psychiatry* 2000; 69:427-30.
61. Brucker AB, Vollert-Rogenhofer H, Wagner M, et al. Heparin treatment in acute cerebral sinus venous thrombosis: a retrospective clinical and MR analysis of 42 cases. *Cerebrovasc Dis* 1998; 8:331-7.
62. Chaluopka JC, Mangla S, Huddle DC. Use of mechanical thrombolysis via microballoon percutaneous transluminal angioplasty for the treatment of acute dural sinus thrombosis: case presentation and technical report. *Neurosurgery* 1999; 45:650-6.
63. Bouser MG. Cerebral venous thrombosis: nothing, heparin, or local thrombolysis. *Stroke* 1999; 30:481-3.
64. Ekseth K, Bostrom S, Vegfors M. Reversibility of severe sagittal thrombosis with open surgical thrombectomy combined with local infusion of tissue plasminogen activator: technical case report. *Neurosurgery* 1998; 43:960-5.
65. Stan J, Lensing AW, Vermeulen M, et al. Heparin treatment for cerebral venous and sinus thrombosis. *Lancet* 1991; 338:597-600.
66. Barnwell SL, Higashida RT, Halbach VV, et al. Direct endovascular thrombolytic therapy for dural sinus thrombosis. *Neurosurgery* 1991; 28:135-42.

67. Horowitz M, Purdy P, Unwin H, et al. Treatment of dural sinus thrombosis using selective catheterization and urokinase. *Ann Neurol* 1995; 38:58-67.
68. Kim SY, Suh JH. Direct endovascular thrombolytic therapy for dural sinus thrombosis: infusion of alteplase. *AJNR Am J Neuroradiol* 1997; 18:639-45.
69. Sobel BE, Gross RW, Robinson AK. Thrombolysis, clot selectivity, and kinetics. *Circulation* 1984; 70:160-164.
70. J F T M de Bruijna, R J de Haanb, J Stam Clinical features and prognostic factors of cerebral venous sinus thrombosis *Neurol Neurosurg Psychiatry* 2001;70:105-108.
71. Ameri A, Bousser MG. Cerebral venous thrombosis. *Neurol Clin* 1992; 10: 87-111.
72. Ferro JM, Lopes MG, Rosas MJ, Femo MA, Fontes J: Long-Term Prognosis of Cerebral Vein and Dural Sinus Thrombosis. Results of the venoport study. *Cerebrovasc Dis* 2002; 13:272-278
73. Pillai LV, Ambike DP, Nirhale S, Husainy SMK, Pataskar S, et al. Cerebral venous thrombosis: An experience with anticoagulation with low molecular weight heparin. *Indian J Crit Care Med* 2005; 9:14-18.
74. Carrol JD, Lead D and Lee HA. Cerebral thrombo phlebitis in pregnancy and puerperium. *QJ med* :35:347 [7].
75. Srinivasan K, Natarajan M. Cerebral Venous And Arterial Thrombosis In Pregnancy and puerperium. *Neurological India* 1974;22:131.
76. Nagaraja D, Taly AB, puerperal cerebral venous thrombosis. *progress in clinical neuro science* 1986;165-177.

77. J.C. Corvol, MD, C. Oppenheim, MD, R. Manai, MD; M. Logak, Diffusion weighted magnetic resonance imaging in a case of cerebral venous thrombosis. Stroke 1998; 29: 2652-59.
78. Keller E, Flacke S, Urbach H, et.al: Diffusion- and perfusion weighted magnetic resonance imaging in deep cerebral venous thrombosis. Stroke 1999; 30:1144-46.
79. Atlas SW, Dubois P, Singer MB, Lu D. Diffusion measurement in intracranial hematoma: Implications of MR imaging in acute stroke. AJNR 2000;21:1190-94.
80. Hermier M, Nighoghossian N. Contribution of susceptibility-weighted imaging to acute stroke assessment. Stroke. 2004;35:1989-94.
81. Puneet Mittal, Vishal Kalia and Sarika Dua Pictorial essay: Susceptibility-weighted imaging in cerebral ischemia. Indian J Radiol Imaging. 2010 Nov; 20(4): 250-253.



# **ANNEXURE 1**

## **INFORMED CONSENT FORM**

I, Mr/Miss/Mrs \_\_\_\_\_,

have been invited to participate in project titled **“ROLE OF MAGNETIC RESONANCE VENOGRAM, DIFFUSION AND SUSCEPTIBILITY WEIGHTED IMAGING IN DIAGNOSIS OF CEREBRAL VENOUS THROMBOSIS”**. It has been communicated to me in my vernacular language about the purpose of the study and the associated possible complications.

My participation in this research project is purely voluntary. I am also aware that I can withdraw from the project at any point of time without citing any reasons whatsoever.

I also agree to co-operate with him and agree by my own free will and in complete consciousness without any influence hereby I give my consent.

**NAME AND SIGNATURE / THUMBPRINT.**

# **ANNEXURE 2**

## **PROFORMA**

**NAME:**

**AGE:**

**SEX:**

**I.P.No.:**

**Address:**

**D.O.A:**

**D.O.D:**

**MRI No.:**

**Occupation:**

**HISTORY OF PRESENT ILLNESS:**

**COMPLAINTS:**

1. Headache
2. Seizures
3. Vomiting
4. Giddiness
5. Focal neurological deficits
6. Coma and impairment of consciousness

**PERSONAL HISTORY:**

1. Intake of alcohol and smoking
2. Oral contraceptive intake
3. Hormone replacement therapy
4. Pregnancy
5. Puerperium

**CLINICAL DIAGNOSIS:**

**MRI FINDINGS:**

PATIENT'S NAME	HOSPITAL NO.	DWI FINDINGS	ADC VALUES	SWI FINDINGS	SINUSES INVOLVED ON MRV

**FINAL DIAGNOSIS:**

# **ANNEXURE 3**

MASTER CHART																				
SL. NO.	NAME	SEX	AGE	HOSPITAL NUMBER	2D TOF MRV-SINUSES INVOLVED										INFARCT		ICH	RESTRICTION ON DWI	ADC VALUES AT ONSET (X1/1000 mm²/s)	BLOOMING ON SWI
					SSS	ISS	St.S	TS	CS	VOG	Cor. Vs	Sig. S	IJV	HAEMORRHAGIC	NON-HAEMORRHAGIC					
1	SANDHYA	F	18	13889	+	-	-	+	-	-	-	+	-	+	-	+	↓ (0.63)	+		
2	RUKMANIYAMMA	F	45	16447	-	-	+	-	-	-	-	-	-	+	-	+	↓ (0.352)	+		
3	SYED REHMAN	M	55	18645	-	-	-	+	-	-	-	-	-	+	-	+	↑ (1.007)	+		
4	NARAYANAMMA	F	52	18803	+	-	-	+	-	-	-	+	-	+	-	+	↑ (0.97)	+		
5	SHANKARAPPA	M	40	25999	-	-	-	+	-	-	-	-	+	-	+	+	↑ (1.51)	-		
6	NARAYANSWAMY	M	60	21980	+	-	+	-	-	-	-	+	-	-	-	-	↑ (1.74)	+		
7	MUNIRAJ	M	43	967043	-	-	-	+	-	-	-	-	+	+	-	+	↓ (0.428)	+		
8	RAMADEVI	F	30	994221	+	-	-	-	-	-	-	-	-	-	+	+	↓ (0.56)	-		
9	BALKESH JAN	F	65	1004222	-	-	+	+	-	-	-	-	-	-	+	+	↓ (0.531)	-		
10	SHANKARI	F	38	834775	-	-	-	+	-	-	-	-	-	-	+	+	↑ (0.48)	-		
11	SOWMYA	F	28	1005770	+	-	+	-	-	-	-	-	-	+	-	+	↓ (0.63)	+		
12	KRISHNAPPA	M	61	1005427	+	-	-	+	-	-	-	+	-	+	-	+	↓ (0.307)	+		
13	NARAYANAMMA	F	42	908957	-	+	+	-	-	-	-	-	-	-	+	+	↑ (0.43)	-		
14	DEVINDRA	M	40	3704	+	-	+	-	-	-	-	-	-	-	-	-	↓ (0.148)	+		
15	RAMACHANDRAPPA	M	65	3564	-	-	-	-	-	+	-	-	-	-	-	+	↓ (0.365)	-		
16	SUDHA	F	20	6270	-	-	-	+	-	-	-	+	-	+	-	+	↑ (1.284)	+		
17	KANYAKUMARI	F	45	13866	+	-	+	-	-	-	-	-	-	+	-	+	↓ (0.423)	+		

18	SHANKAR	M	30	11770	+	-	-	+	-	-	-	-	-	-	-	-	+	-	↓ (0.62)	-
19	JAYANTHI	F	38	15362	-	-	-	-	+	+	-	-	-	-	-	-	-	+	↑ (0.94)	+
20	THIMARAJU	M	56	19620	-	-	-	+	-	-	-	-	-	-	-	-	+	+	↑ (0.856)	-
21	GIRI BABU	M	28	991077	-	-	+	-	-	-	-	-	-	-	-	-	-	+	↑ (0.88)	+
22	ANITHA	F	19	129323	+	-	-	+	-	-	-	-	-	-	-	-	+	+	↑ (0.92)	-
23	RAGHUPATHY	M	63	131791	+	-	-	+	-	-	-	-	-	-	-	-	+	+	↑ (0.90)	-
24	SRINIVAS	M	35	133490	+	-	-	-	-	+	-	-	-	-	-	-	-	-	↓ (0.327)	+
25	ANJAPPA	M	35	138834	-	-	+	-	-	+	-	+	-	-	-	-	-	+	↑ (1.31)	+
26	SWETHA	F	12	995812	+	-	-	-	-	-	-	-	-	-	-	-	+	+	↓ (0.68)	+
27	SHAHANA	F	35	198887	+	+	+	-	-	-	-	-	-	-	-	-	+	+	↓ (0.56)	-
28	SHOBHA	F	23	192250	-	-	-	+	-	-	-	-	+	-	-	-	-	-	↓ (0.47)	+
29	MAHESH	M	27	146454	-	-	-	-	-	+	+	-	-	-	-	-	-	+	↑ (0.97)	+
30	VENKATAMMA	F	70	146617	+	-	-	+	-	-	-	-	-	-	-	-	+	+	↓ (0.465)	-
31	LAKSHMAN REDDY	M	65	158042	-	-	-	+	-	-	-	-	-	-	-	-	-	+	↑ (0.980)	+
32	ZAFFARUNNISA	F	75	161195	-	-	-	+	+	-	-	-	-	+	-	-	+	+	↑ (0.90)	-
33	ZAINA TABASSUM	F	18	165316	-	+	-	+	-	-	-	+	-	-	-	-	+	+	↓ (0.74)	+
34	GOWRAMMA	F	47	168033	-	-	-	-	-	+	-	-	-	-	-	-	-	+	↓ (0.39)	+



## **LIST OF ABBREVIATIONS IN MASTERCHART**

ICH- Intracerebral Hematoma

SSS- Superior sagittal sinus

ISS- Inferior sagittal sinus

St. S- Straight sinus

TS- Transverse sinus

CS- Cavernous sinus

VOG- Vein of Galen

Cor Vs- Cortical veins

Sig S-Sigmoid sinus

IJV- Internal jugular vein

DWI- Diffusion weighted images

SWI- Susceptibility weighted images

ADC- Apparent diffusion coefficient